AD-A136 978 THE CENTRIFUGAL SIMULATION OF BLAST PARAMETERS(U) NEW MEXICO ENGINEERING RESEARCH INST ALBUQUERQUE J P NIELSEN DEC 83 NMERI-TA2-2 AFESC/ESL-TR-83-12 1/1

UNCLASSIFIED F29601-81-C-0013 F/G 19/4 NL

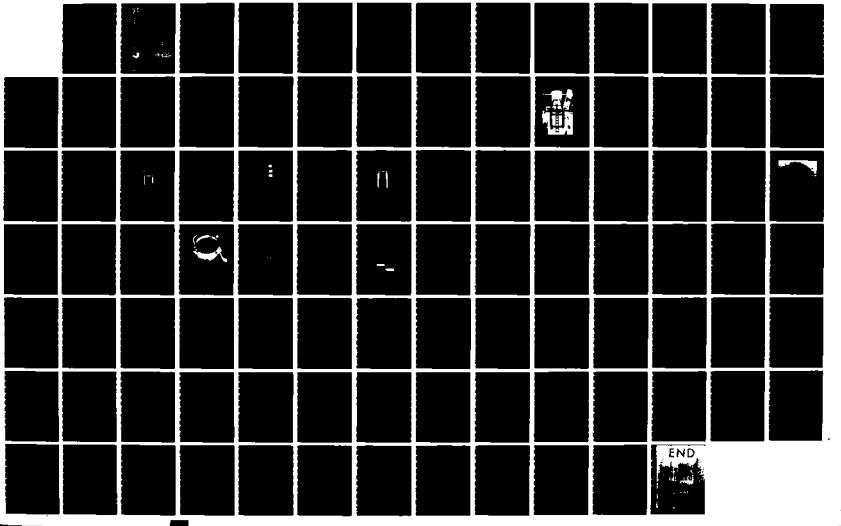

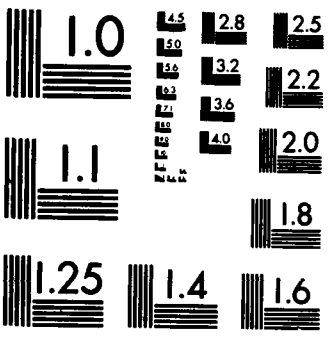

MICROCOPY RESOLUTION TEST CHART
NATIONAL BUREAU OF STANDARDS-1963-A

(12)

ESL-TR-83-12

AD A136978

THE CENTRIFUGAL SIMULATION OF BLAST PARAMETERS

JOHN P. NIELSEN, PhD.

NEW MEXICO ENGINEERING RESEARCH INSTITUTE
UNIVERSITY OF NEW MEXICO, BOX 25
UNIVERSITY STATION, ALBUQUERQUE, NEW MEXICO

DECEMBER 1983

FINAL REPORT
27 FEBRUARY 1981 - 1 JUNE 1983

APPROVED FOR PUBLIC RELEASE; DISTRIBUTION UNLIMITED

AFESC

ENGINEERING AND SERVICES LABORATORY
AIR FORCE ENGINEERING AND SERVICES CENTER
TYNDALL AIR FORCE BASE, FLORIDA 32403

NOTICE

PLEASE DO NOT REQUEST COPIES OF THIS REPORT FROM HQ AFESC/RD (ENGINEERING AND SERVICES LABORATORY). ADDITONAL COPIES MAY BE PURCHASED FROM:

NATIONAL TECHNICAL INFORMATION SERVICE
5285 PORT ROYAL ROAD
SPRINGFIELD, VIRGINIA 22161

FEDERAL GOVERNMENT AGENCIES AND THEIR CONTRACTORS REGISTERED WITH DEFENSE TECHNICAL INFORMATION CENTER SHOULD DIRECT REQUESTS FOR COPIES OF THIS REPORT TO:

DEFENSE TECHNICAL INFORMATION CENTER
CAMERON STATION
ALEXANDRIA, VIRGINIA 22314

UNCLASSIFIED

SECURITY CLASSIFICATION OF THIS PAGE *(When Data Entered)*

REPORT DOCUMENTATION PAGE		READ INSTRUCTIONS BEFORE COMPLETING FORM
1. REPORT NUMBER ESL-TR-83-12	2. GOVT ACCESSION NO. AD-A136 978	3. RECIPIENT'S CATALOG NUMBER
4. TITLE *(and Subtitle)* THE CENTRIFUGAL SIMULATION OF BLAST PARAMETERS		5. TYPE OF REPORT & PERIOD COVERED Final Report for Period 27 Feb. 81 through 1 June 83
		6. PERFORMING ORG. REPORT NUMBER NMERI TA2-2
7. AUTHOR(s) John P. Nielsen, Ph.D.		8. CONTRACT OR GRANT NUMBER(s) F29601-81-C-0013
9. PERFORMING ORGANIZATION NAME AND ADDRESS New Mexico Engineering Research Institute University of New Mexico, Box 25, University Station, Albuquerque, New Mexico 87131		10. PROGRAM ELEMENT, PROJECT, TASK AREA & WORK UNIT NUMBERS PE: 62601F JON: 26730001
11. CONTROLLING OFFICE NAME AND ADDRESS Engineering and Services Laboratory Air Force Engineering and Services Center Tyndall Air Force Base, Florida 32403		12. REPORT DATE December 1983 13. NUMBER OF PAGES 92
14. MONITORING AGENCY NAME & ADDRESS *(if different from Controlling Office)*		15. SECURITY CLASS. *(of this report)* Unclassified 15a. DECLASSIFICATION/DOWNGRADING SCHEDULE

16. DISTRIBUTION STATEMENT *(of this Report)*

Approved for public release; distribution unlimited.

17. DISTRIBUTION STATEMENT *(of the abstract entered in Block 20, if different from Report)*

18. SUPPLEMENTARY NOTES

Availability of this report is specified on reverse of front cover.

19. KEY WORDS *(Continue on reverse side if necessary and identify by block number)*

Weapon Simulation
Blast Pressures
Simulation
Centrifuge Testing
Dimensional Analysis
Burster Slabs
Stress Gages

20. ABSTRACT *(Continue on reverse side if necessary and identify by block number)*

This study is concerned with the use of a centrifuge as an experimental device on which free-field blast parameters could be evaluated. Free-field normal stress, created by the detonation of simulated high-explosive charges, was recorded within a sand medium. A series of experiments was concerned with the measurement of free-field normal stress, created by exploding buried charges. Another test series was concerned with the free-field normal stress

DD FORM 1 JAN 73 1473 EDITION OF 1 NOV 65 IS OBSOLETE

UNCLASSIFIED

SECURITY CLASSIFICATION OF THIS PAGE *(When Data Entered)*

No. 20 ABSTRACT (Concluded)

beneath a concrete burster slab. The results of this study indicate that a centrifuge can be used as a simulator on which free-field blast effects can be evaluated.

PREFACE

This report was prepared by the New Mexico Engineering Research Institute, University of New Mexico, at the Eric H. Wang Civil Engineering Research Facility, Kirtland Air Force Base, New Mexico, under Contract F29601-81-C-0013, Job Order 26730001, for the Engineering and Services Laboratory, Headquarters Air Force Engineering and Services Center (AFESC/RD), Tyndall Air Force Base, Florida.

This report summarizes work done between 27 February 1981 and 1 June 1983. Capt Paul L. Rosengren, Jr., was the AFESC/RDCS Project Officer.

This report has been reviewed by the Public Affairs Office (PA) and is releaseable to the National Technical Information Service (NTIS). At NTIS it will be available to the general public, including foreign nationals.

This technical report has been reviewed and is approved for publication.

Paul L. Rosengren Jr.
PAUL L. ROSENGREN, JR., Capt, USAF
Project Officer

PAUL Y. THOMPSON, PhD
Tech Base Program Manager

John E. Goin
JOHN E. GOIN, Lt Col, USAF
Chief, Engineering Research Division

Robert E. Brandon
ROBERT E. BRANDON
Deputy Director
Engineering and Services Laboratory

Accession For	
NTIS GRA&I	☒
DTIC TAB	☐
Unannounced	☐
Justification	
By	
Distribution/	
Availability Codes	
Dist	Avail and/or Special
A-1	

(The reverse of this page is blank)

TABLE OF CONTENTS

TABLE OF CONTENTS (Concluded)

LIST OF FIGURES

LIST OF FIGURES (Concluded)

LIST OF TABLES

SECTION I
PRELUDE

INTRODUCTION

This report documents a study concerned with the use of a centrifuge as an experimental device on which free-field blast parameters could be evaluated. The centrifugal-simulation of high-explosive (HE) charges was investigated as a means of improving the present techniques used to predict free-field blast parameters. The blast parameters of interest included normal stress, particle velocity, and acceleration.* However, because of a lack of suitable accelerometers and velocity gages, this study is concerned only with normal stress.

The gravity field created by the rotating centrifuge increase the effective body force of gram-weight charges, thus simulating a larger explosive. The prototype explosive is a cylindrical-shaped , cased explosive embedded in a concrete burster slab. The prototype burster slab is supported by a deep stratum of sand. A definition of the variation of normal stress in respect to distance in the region near the explosive was a primary goal of this study.

BACKGROUND

Recent developments in precision-guided, conventional weapons have greatly increased the vulnerability of military facilities. It is now possible for an attacker to precisely deliver relativly large conventional weapons on selected targets. One means of protecting strategic facilities from such weapons is a concrete burster slab and intervening sand stratum. Not only can weapons be accurately directed at these sites, but contemporary weapons can penetrate part of the burster slab before detonating. Economic

---

*In this report the term pressure refers to the detonation pressure of an explosive. The pressure in the free field as a result of detonating the weapon is referred to as stress. No distinction is made between hydrodynamic or soil stress.

design and survival of buried structures requires a thorough knowledge of the stress loadings created by the weapon when it detonates. The assumption is made that the burster slab defeats the weapon; that is, the weapon lodges in the burster slab and then detonates.

Extensive theoretical and experimental research was performed after World War II (Reference 1) to describe HE-generated blast waves and their propagation and attenuation through various media. However, much of that work involved the use of spherical, uncased, surface-detonated charg Moreover, most of the data associated with those early tests were collect at relatively large-scaled distances (λ) because of the instrumentatio difficulties associated with the near field, $\lambda < 2$. Most of the work done d in the 1950s and 1960s was in the field of nuclear (or HE simulation of nuci blast environments. Virtually none of these programs included a burster slab, and only a few of the tests included cased explosives. Model tests (circa 1980) have indicated that cased explosives which were detonated within a burster slab did not yield normal stress attenuation rates consistent with those extrapolated from the studies mentioned above.

PURPOSE

The purpose of the effort documented in this report was to develop an experimental technique to define the free-field blast parameters in the region near cylindrical-shaped, cased, HE charges, in soil and concrete-soil media.

SCOPE

To conduct this research it was necessary to (1) review the current state of the art regarding the definition of blast wave generation and propagation through soil and concrete-soil media, (2) define the parameters necessary to describe such phenomena, (3) review the experimental techniques currently employed for such studies, (4) examine the scaling laws related to blast wave propagation, and (5) critically evaluate the instrumentation and data acquisition systems used in these types of studies. Subsequent to these reviews, the experimental technique recommended to meet the purpose of this study was to be evaluated.

CRITERIA

The experimental technique recommended to satisfy the objectives of this study was required to have the following capabilities:

1. Must allow for variation of charge weight. The maximum scaled charge could not exceed 15 pounds of trinitrotoluene (TNT) to simulate a full-scale TNT charge weight of 1000 pounds.

2. Must allow variation of the depth of burial up to a scaled distance of 3 feet.

3. Must allow variation of the charge orientation from the normal to an angle of 60 degrees.

4. Must allow variation of the scaled thickness of the prototype concrete burster slab ranging from 3 to 6 feet.

5. Must allow representation of the concrete-soil media as a half space.

6. Must provide quantifiable data on the blast parameters in the scaled distance range of 0.5 to 2 in the soil and concrete soil media.

7. Must be repeatable or reusable with minor refurbishing.

APPROACH

The initial effort in this research was principally concerned with a critical review of blast parameter evaluation techniques with respect to their potential to meet the full range of capabilities outlined above. During a briefing held at the Air Force Engineering and Services Center on 1 April 1981, the author outlined several potential experimental techniques that could be used as simulators. These included a modified Stanford Research Institute (SRI) single-source line loader, small-charge field tests, very small-charge model tests, and the use of a centrifuge. Of these techniques, only the centrifugal concept had the potential to meet all of the preceding criteria.

Following that briefing, the scope of this project was extended to include an experimental evaluation of the centrifugal concept. This report

documents that study. Section II of this report is a discussion of the appropriate scaling laws derived for gravity scaling. All aspects of the experimental phase--pressure gage development, data acquisition, model explosives, system modeling, and an outline of the experimental program--are discussed in Section III. Experimental results are presented in Section IV. Section V is a discussion of those results. An extensive bibliography is included at the end of this report.

SECTION II
DIMENSIONAL ANALYSIS AND SIMILITUDE

DIMENSIONAL ANALYSIS

The techniques of dimensional analyses are used in experimental programs in which the difficulty encountered in developing a closed-form solution (differential equation) which describes the phemonena is so complex as not to be readily discernible. At best, such equations (when they can be developed) are based upon first-order concepts. Thus parametric studies based upon differential equations suggest significantly different system behavior than that observed experimentally. This departure is due to the imperfection of human observations (objective uncertainty), the imperfection of intellectual concepts devised to reproduce physical phenomena (subjective ignorance), unrealistic mathematical assumptions (used to ease the computational effort), and experimental error in the test program. Error in the test program exists regardless of the analyses employed. However, it is more difficult to identify error when the data are interpreted using first-order concepts.

Subjective ignorance disappears in the formulation of a problem based upon the concepts of dimensional analysis. This is because the functional form of the relationship between the dependent and independent variables is determined experimentally. Thus the weakness of dimensional analysis is immediately obvious; a class or family of solutions (parametric studies) cannot be generated as in the case of closed-form solutions. Rather, each functional relationship must be determined through experimentation.

Objective uncertainty also exists in dimensional analysis, but the incompleteness that such uncertainty suggests is immediately obvious in an examination of the experimental data. Thus, once the possibility of significant constant or systematically changed errors is identified and removed from the experiment or minimized, and the remaining errors are primarily random, the deficiencies in the model due to objective uncertainty can be identified.

By the simple process of considering additional independent variables the model can be revised, as often as necessary, until a satisfactory correlation

is achieved between the dependent variable and the independent variables. The process is actually one of eliminating objective uncertainty from the analysis. In a sense, dimensional analysis contains a feedback mechanism which permits the analyst to eventually identify the significant variables in the problem under consideration. In short, the technique greatly minimizes objective uncertainty. The converse is the situation in closed-form solutions. In these cases, experimental data always depart from the mathematical model because of random errors in the test procedures and, more importantly, because the functional relationship was established a priori. In essence, the researcher uses an incomplete theory to describe a physical event. The data from the physical event are manipulated to conform to the incomplete concept (objective uncertainty), and, in so doing, the behavior of the event is modified by subjective ignorance. The physical system is forced to respond in a manner that is not compatible with its essential boundary conditions or intensive material properties. The great tragedy is that the results of these force fits often become engineering standards. Hopefully, none of the existing strategic facilities designed on the basis of these standards will ever be put to the test.

Figure 1 is an orthogonal view of the prototype burster-slab sand system. Also shown is the centrifugal model of the system. An immediately obvious problem with the model is that its boundaries provide a surface for reflection of the explosive-induced pressure wave. The size of the model is limited to space provided on the centrifuge test platform. Because the boundary is necessary, data traces will need to be examined for boundary effects.

The primary dependent parameter of interest in this study is normal stress σ, $(ML^{-1}T^{-2})$. Other possible dependent parameters are acceleration, particle velocity, displacement, or characteristic time. A list of the assumed (objective uncertainty) independent parameters is presented in Table 1.

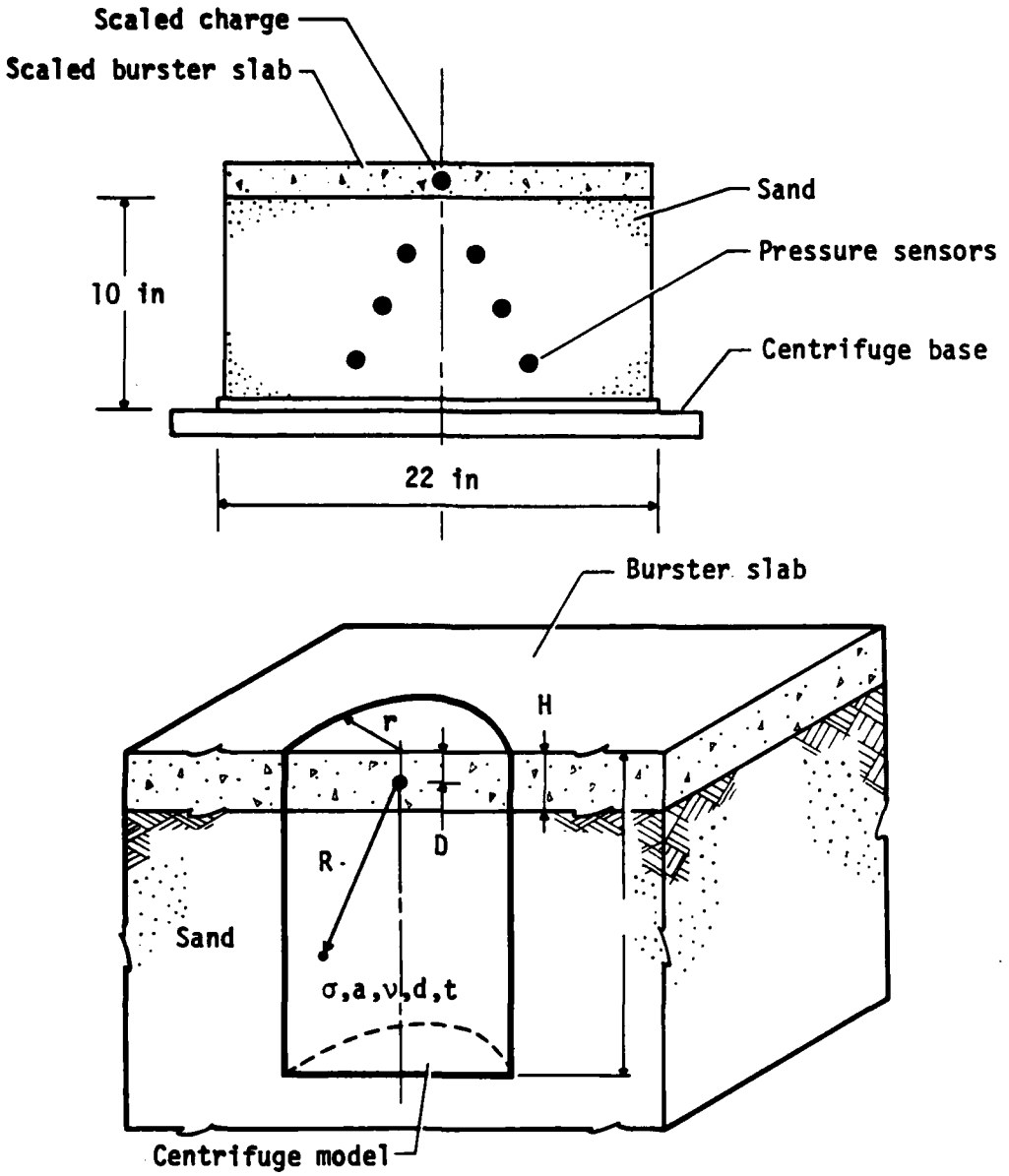

Figure 1. Prototype System and Centrifuge Model.

TABLE 1. INDEPENDENT PARAMETERS FOR THE CENTRIFUGAL MODELING OF BLAST PRESSURE.

Parameter	Description	Dimensions
Explosives	Energy, E_o	ML^2T^{-2}
	Pressure, P_o	$ML^{-1}T^{-2}$
	Depth of Burial, D	L
Burster-Slab	Thickness, H	L
	Mass Density, ρ_1	ML^{-3}
	Dilatational Wave Speed, C_1	LT^{-1}
	Poisson's Ratio, μ_1	---
	Strength, α_1	$ML^{-1}T^{-2}$
Soil (Sand)	Mass Density, ρ_2	ML^{-3}
	Dilatational Wave Speed, C_2	LT^{-1}
	Poisson's Ratio, μ_2	---
	Strength Parameter α_2	$ML^{-1}T^{-2}$
Other Parameters	Gravity, G	LT^{-2}
	Bucket Dimensions, r,d	L
	Range	L

The Buckingham π-theorem (Reference 2) is fundamental to the concept of dimensional analysis. The π-theorem is adequately presented in countless books concerned with hydraulics and fluid mechanics; its implementation is not presented here, only the results. An excellent treatment of the π-theorem applied to ground motion problems is included in Reference 3. It is sufficient to state that by means of the π-theorem the independent parameters are formed into ratios, called π-terms. A significant aspect of each π-term is that it is a nondimensional term. Each term is an independent variable ratio which, when combined with all other π-terms, defines the functional relationship between the dependent and independent variables. Thus, nondimensional stress is expressed as

$$\frac{\sigma}{P_o} = F\left[\zeta\left(\frac{P_o}{E_o}\right)^{1/3}, \frac{P_o}{\rho C^2}, \mu, \frac{C_1}{C_2}, \frac{\zeta_1}{\zeta_2}, \frac{\alpha_1}{\alpha_2}, \frac{G}{C^2}\left(\frac{E_o}{P_o}\right)^{1/3}, \ldots\right] \quad (1)$$

where ζ_1, or ζ_2, is any characteristic length, such as radial position, burster-slab thickness, any dimension of the explosive, or any other characteristic length. The dots indicate that Equation (1) is not complete. Completeness might be achieved by the addition of π-terms made up of such variables as sand moisture, viscosity, or strain-rate effects. The concept of objective uncertainty is readily admitted to this point. Only an experimental exercise will produce the data to define the functional form of Equation (1); and an analysis of variance will suggest the need for additional terms in the equation.

SIMILITUDE

For data from model tests to be useful in predicting prototype behavior, invariance must exist between the model and the prototype. Because a model is used, it becomes obvious that its dimensions must be proportional (similar) to those of the prototype. The scaling relationships used to provide similarity between the model and prototype are derived from dimensional analysis. Similitude involves scaling not only characteristic lengths (dimensions) but also time, material properties, and, in the case of this study, gravity. Thus any characteristic length related to the prototype is divided by n to yield the corresponding dimension for the model.* The scaling relationships derived for this study are presented in Table 2.

These relationships are derived from the π-terms developed through application of the concepts of dimensional analysis. Some of these π-terms are included here to illustrate the concept.

$$\pi_1 = \frac{\sigma}{\rho_2 C_2^2} \qquad \text{Equivalency of stress}$$

$$\pi_2 = \zeta \left(\frac{\rho_0}{E_0} \right)^{1/3} \qquad \text{Geometric similarity of charateristic length}$$

$$\pi_3 = \frac{\alpha}{\rho C^2} \qquad \text{Similarity of medium properties}$$

*In this report n is the ratio of the centrifugal acceleration to the gravitational field at the earth's surface. For simplicity this ratio is called the G-level, implying n = 10 if the centrifugal acceleration is 322 ft/s^2.

TABLE 2. SCALING RELATIONSHIPS FOR GRAVITY SCALING.

Quantity	Full Scale	Model Scale
Linear Dimension	1	$1/n$
Area	1	$1/n^2$
Volume	1	$1/n^3$
Time	1	$1/n$
Velocity	1	1
Acceleration	1	n
Mass	1	$1/n^3$
Force	1	$1/n^2$
Energy	1	$1/n^3$
Stress	1	1
Strain	1	1
Density	1	1

$$\pi_4 = \frac{G}{C^2}\left(\frac{E_0}{P_0}\right)^{1/3} \qquad \text{Gravity scaling of blast energy}$$

$$\pi_5 = Ct\left(\frac{P_0}{E_0}\right)^{1/3} \qquad \text{Gravity scaling of time}$$

Eighteen π-terms are associated with the independent parameters listed in Table 1 and the five response (dependent) parameters. The scaling factors presented in Table 2 are developed from these π-terms.

Considering gravity scaling of energy for example:

$$\frac{G}{C^2}\left(\frac{E_0}{P_0}\right)^{1/3} = \frac{nG}{C^2} \cdot \frac{1}{n}\left(\frac{E_0}{P_0}\right)^{1/3} = \frac{nG}{C^2}\left(\frac{E_0}{n^3}\right)^{1/3}\left(P_0\right)^{-1/3}$$

Therefore, energy scales as $1/n^3$.

The π-term of importance to this project is π_4. This term can be written in terms of mass as

$$\pi_4 = \frac{G}{Q}\left(\frac{W}{\delta}\right)^{1/3} \qquad (2)$$

where

Q = heat of detonation per unit mass of explosive
δ = initial density of the explosive
W = mass of the explosive
G = gravity

By equating the π_4-term of the model to that of the prototype, the similitude requirement for explosives can be developed. This development is discussed in Section III, Explosives. Further details on modeling are also presented in Section III, Experimental Program.

(The reverse of this page is blank.)

SECTION III
EXPERIMENTAL PROCEDURES

INTRODUCTION

The experimental phase of this study consisted of detonating a small explosive charge embedded in a model burster slab and recording the free-field normal stress at selected locations in a contiguous sand medium. The burster slab and sand continuum were contained in a 22-inch diameter by a 12-inch high aluminum test fixture which was mounted on the test platform on a 30,000 G-lb centrifuge. The explosive charge was detonated with the centrifuge rotating at a predetermined constant angular velocity. The gravity field which develops because of the rotational effects of the centrifuge increases the effective body force of gram-weight charges, thus simulating a larger explosive. This technique permits the yield of a small explosive to simulate that of a large explosive. The benefits of such an approach are obvious. A series of 22 of these experiments was performed as described later in this section.

To perform these experiments it was necessary to (1) become familiar with the centrifuge and its operation, (2) develop safety procedures relative to its operation and the detonation of the explosives, (3) establish the geometry and weight of each explosive, (4) model the burster slab and sand media, and (5) develop a suitable stress gage and associated data acquisition system.

CENTRIFUGE

The centrifuge used to conduct the experimental phase of this project is a Genisco model E185 (Serial Number 11). A photograph of this centrifuge is presented in Figure 2. The boom is nominally 6 feet long. The centrifuge is situated below floor level in a concrete pit located in Building 1001 on Kirtland Air Force Base. The centrifuge is covered with a reinforced concrete roof with access to the pit through steelplate doors. The centrifuge is controlled by suitable electrical and hydraulic controls located aboveground in a console remote to the centrifuge. The centrifuge was originally built to test aviation electronic and mechanical systems under G-loadings similar to those experienced during flight. A variable-speed hydraulic drive system is used to rotate the centrifuge. The hydraulic power unit is enclosed in the console;

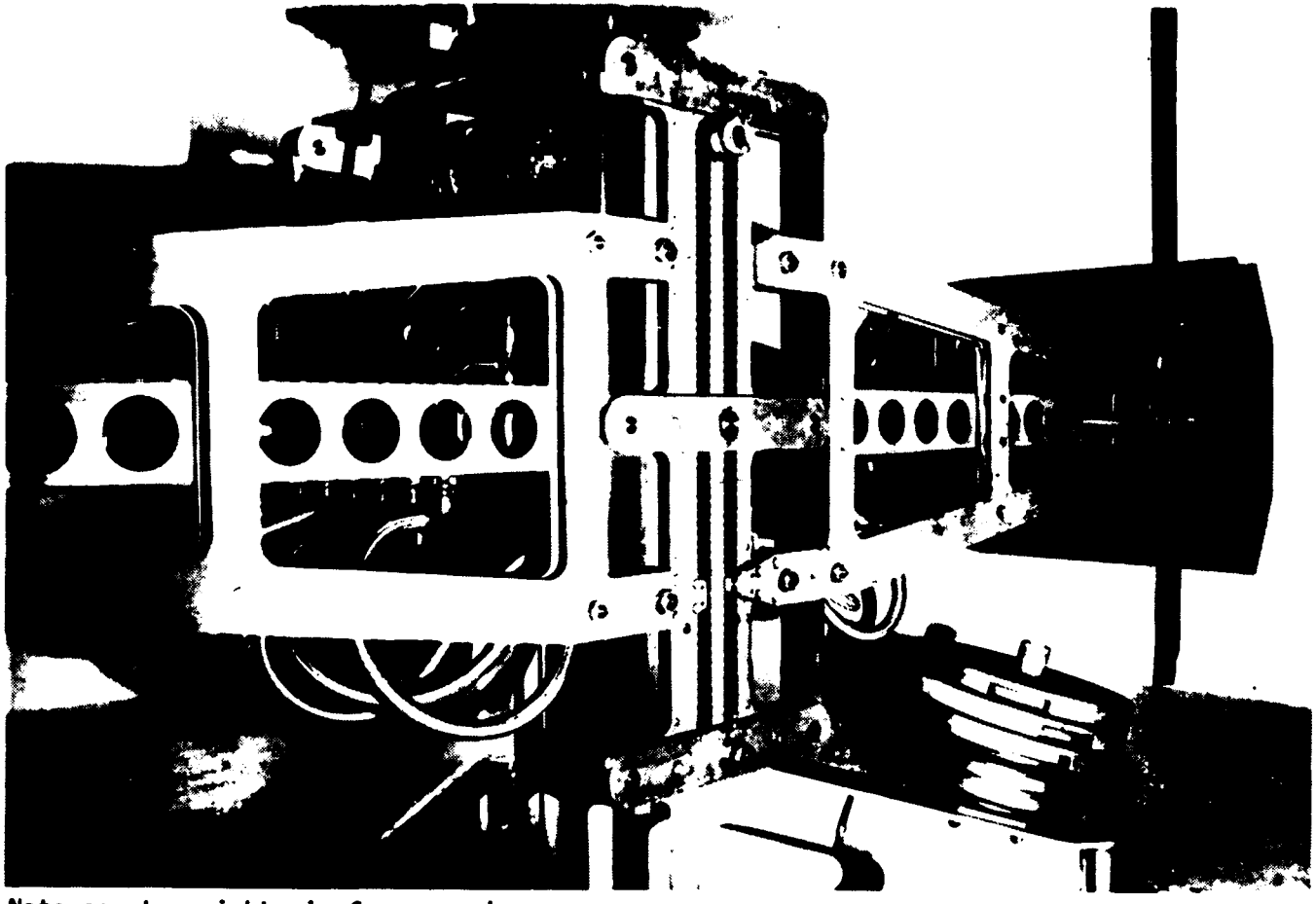

Note counterweights in foreground.

Figure 2. Genisco Centrifuge.

the fluid motor is installed at the bottom of the rotor assembly. The boom consists of two symmetrical cantilever arms, each of which supports a test platform. The platforms are 30 inches square and were designed to operate in one of five fixed positions: horizontal, 45, 90, 135, or 180 degrees (inverted). Electrical interlock switches prevent rotation of the centrifuge unless the platforms are securely locked into one of the specified positions. However, for this research the platforms were modified to permit the centrifuge to operate in the swing-bucket mode rather than fixed-bucket as described. These modifications were made in accordance with the instructions contained in a report prepared by the manufacturer for the New Mexico Engineering Research Institute (NMERI) (Reference 4). The swing-bucket modification was necessary to facilitate handling the test fixture which weighed, on the average, 365 pounds.

In the swing-bucket mode, the test fixture could be easily lowered onto the horizontal test platform and then permitted to swing into the 90-degree position as the centrifuge was subsequently accelerated to a prescribed constant angular velocity. Mechanical scratch gages, mounted on the boom and installed to make contact with one of the arms of the swinging platforms, indicated that the 90-degree position was consistently achieved.

The centrifuge is equipped with 28 slip rings which provide for electrical connections between the rotating test object and the remote control console. The boom is free to pivot approximately 1 degree about a horizontal transverse axis. Static balancing is achieved if identical test objects are placed on each of the opposite test platforms. If a single object is to be tested (as in this research) counterweights are mounted on the opposite test platform. An automatic dynamic balancing feature of the machine eliminates the necessity for static balancing to less than 10 pounds. Wow and drift of the boom assembly during a 1-minute period is less than 0.5 percent of the operating rate at any speed. Speed is indicated on a direct reading magnetic-impulse-type tachometer indicator, accurate to within 1 1/4 percent of full scale. Precision speed indicators are provided by a pulse generator unit and an electronic counter on a four-decade, digital display. Accuracy of the unit is within 0.1 percent at angular velocities above 12 rpm. The average angular speed over a 1- or 10-second interval is indicated directly in revolutions per minute.

Two test objects, each weighing up to 500 pounds, can be tested simultaneously, one on each of the two test platforms. The maximum range of the centrifuge is 100 G at a 72-inch radius, 22 to 220 rpm. infinitely variable. The centrifuge is rated at 30,000 G-lb. Thus, at its maximum centrifugal acceleration (100 G) a load of 300 pounds can be applied to each test platform. An acceleration of 60 G would be the maximum allowed if 500 pounds were applied to each test platform.

SAFETY PROCEDURES

The centrifuge is placed in a circular reinforced concrete pit approximately 7 feet deep. The roof of the pit is also made of reinforced concrete. Several steelplate doors mounted in the roof provide access to the floor of the pit. Thus, personnel are adequately protected from the inadvertent emission of missiles from the rotating centrifuge. Interlock switches on the access doors serve as safety devices. These prevent the rotor assembly from operating when any door is not properly seated against its jam. Conversely, these switches initiate an immediate shutdown of the rotor if an attempt is made to open a door while the centrifuge is rotating. Other similar devices prevent the rotor from exceeding a minimum angular velocity if a dynamic unbalance exists, or if the weight of the test object exceeds 500 pounds. Further details concerning the Genisco centrifuge and its operation or maintenance are contained in Reference 5.

The placement of the test fixture containing the burster slab, with the stress gages embedded in the sand, was under the direction of the project engineer. However, once the fixture was secured to the platform, an ordnance technician served as the test conductor. This person took charge of the operation and served as the responsible safety officer during the arming and detonation of the explosive. This also included a postshot inspection of the centrifuge pit to ensure that the area was free of all explosive hazards. An Explosives Facility License, Reference 6, was granted to the Civil Engineering Research Facility to detonated gram-weight explosives in the centrifuge facility. The approved Centrifuge Countdown Procedure is presented as Appendix A.

EXPLOSIVES

In simulation testing, an attempt is made to maintain similitude between the full-scale object (prototype) and a scaled model of the object. The concept evaluated in this project is based on the consideration that a small explosive charge (model) subjected to an acceleration field can, upon detonation, simulate the effect of a larger explosive (prototype). The centrifuge is used to create the acceleration field. In regard to the prototype explosive, simulation requires that the characteristic dimensions and yield of the model be determined according to the appropriate scaling relationships (Section II). These relationships require that the characteristic lengths of the model scale as the reciprocal of the G-level; and that the energy (yield) scales as the reciprocal of the G-level cubed, with respect to those values for the prototype. Thus, if a particular weapon (prototype) is to be simulated, the application of these scaling relationships yields the necessary dimensions and explosive weight for the model. It is obvious that an infinite number of models exist for a particular weapon if the G-level is infinitely variable as with a centrifuge. This is advantageous because it permits the consideration of a range of models in simulation experiments.

This flexibility is also significant in that it improves the outlook for full experimental similitude when other secondary test parameters are considered. For example, the scaling relationships may suggest that the size of other features included in, or necessary to, the experiment be so small as not to be commercially available, difficult to manufacture or handle, or simply not available. Thus, to perform the intended experiment, the G-level is established on the basis of available, achievable model dimensions, or those of the secondary features of the prototype system. The advantage of an infinitely variable G-field (centrifuge) is that it provides a means of approaching the ideal condition of constructing an experiment that is in compliance with all conditions required for similitude. However, this condition is rarely met, not only because of physical limitations, but because of the analyticity from which the scaling laws are established. By their very nature these laws are subjective in that they are derived through an interrogative process (dimensional analysis) that is highly subjective and admittedly incomplete. The process (dimensional analysis) is used when science admits to its inability to develop an exact mathematical statement for the problem. These

limitations notwithstanding, it is not suggested that the use of dimensional analysis be abandoned. To the contrary, a correctly formulated problem provides insight concerning the parametric relationships which exist between the dependent and perceived independent variables. These relationships serve to improve the understanding of the problem and to suggest experimental and analytical tactics which rarely are achieved through physical reasoning alone. Perfect correlations cannot, however, be expected in experimental observations when the results are formulated in terms of dimensional parameters, because the theory is always incomplete, because full simulation cannot be achieved, and because of experimental errors.

The limitations and considerations discussed above are fully demonstrated in the details leading to the selection of model explosives for use in this project. While a particular weapon (prototype) was not identified with this project, the weapon considered was identified as a general-purpose bomb (GPB) in the total weight range of 500 to 2000 pounds. On the surface, simulation appears easy; application of the appropriate scaling laws to the explosive weight and dimensions of these bombs yields the corresponding values for the model explosive, the G-level known or selected a priori. For example, a 2000-pound GPB containing 1117 pounds of TNT could be simulated by 107, 13, 4, or 1.7 grams of cyclotrimethylenetrinitramine (RDX) when accelerated to 20, 40, 60, or 80 G respectively. However, the actual weight of TNT in any GPB is variable, depending upon the manufacturing processes. These processes affect not only the properties of the TNT, but also influence the shape of the explosive contained within the bomb case. Likewise, the dimensions and shape of the case varies, as well as its intensive properties.

Complete simulation requires a review of all of the above factors. Statistical uncertainties are obviously present in respect to both the intensive and extensive properties of the prototype to be simulated. True dimensional and energy scaling would lead to model charges that would be one of a kind and expensive to fabricate. Not only would the cost of the project be significantly affected, but it is doubtful that such detail, though desirable, would enhance the real purpose of this program, namely, to demonstrate the feasibility of the centrifuge as a simulator to define blast parameters in the region near a high-explosive charge placed in a concrete-soil medium.

An alternate approach was taken, though it was still guided by the appropriate scaling laws. This consisted of dealing with what could be considered the average properties of general-purpose bombs. The first consideration was that of determining the weight of a model RDX charge, expressed as a function of the G-level, required to simulate a particular general-purpose bomb. Equation (2) was used for this purpose. The results of these computations are shown in Table 3.

TABLE 3. THEORETICAL MODEL EXPLOSIVE SIMULATION WEIGHTS.

Bomb Designation, pound	20 g	40 g	60 g	80 g	100 g
	Weight of RDX in grams				
250	12.35	1.54	0.46	0.19	0.10
500	25.57	3.20	0.95	0.40	0.20
1000	53.43	6.68	1.98	0.83	0.43
2000	106.95	13.37	3.98	1.67	0.86

These results, based upon similitude concepts, indicate that small charges, when subjected to the indicated acceleration, can simulate the yield of large weapons. Because of the uncertainties related to centrifuge explosive testing, the NMERI Safety Officer established a 1-gram limit to the output charge of any model explosive. Adherence to this condition was part of the previously mentioned license (Reference 6). Accordingly, the test conditions under which each of the bombs could be simulated are the particular combinations of accelerations and mass lying above the bold line in Table 3. Table 4 lists the theoretical dimensions for the model charges listed above the bold line in Table 3.

A review of the results presented in Tables 3 and 4 leads to the conclusion that these data are somewhat representative of commercially available detonators, such as the Reynolds RP-83 detonator shown in Figure 3. This standard detonator consists of an exploding wire bridge (1), a low density pressing of pentaerythritol tetranitrate (PETN) (2), a high-density RDX initiator (3), and a high-density RDX output charge (4), all of which are contained in a 0.007-inch thick aluminum cup (5). The high-density output charge

TABLE 4. THEORETICAL DIMENSIONS OF MODEL EXPLOSIVES.

Bomb Designation, pound	60 g	80 g	100 g
	Diameter, inch		
250	0.17	0.13	0.10
500	0.23	0.17	0.14
1000	----	0.22	0.18
2000	----	----	0.22
	Height, inch		
250	0.45	0.34	0.27
500	0.54	0.41	0.33
1000	----	0.50	0.40
2000	----	----	0.51
	Case Thickness, inch		
250	0.005	0.003	0.003
500	0.005	0.004	0.003
1000	-----	0.006	0.005
2000	-----	-----	0.005

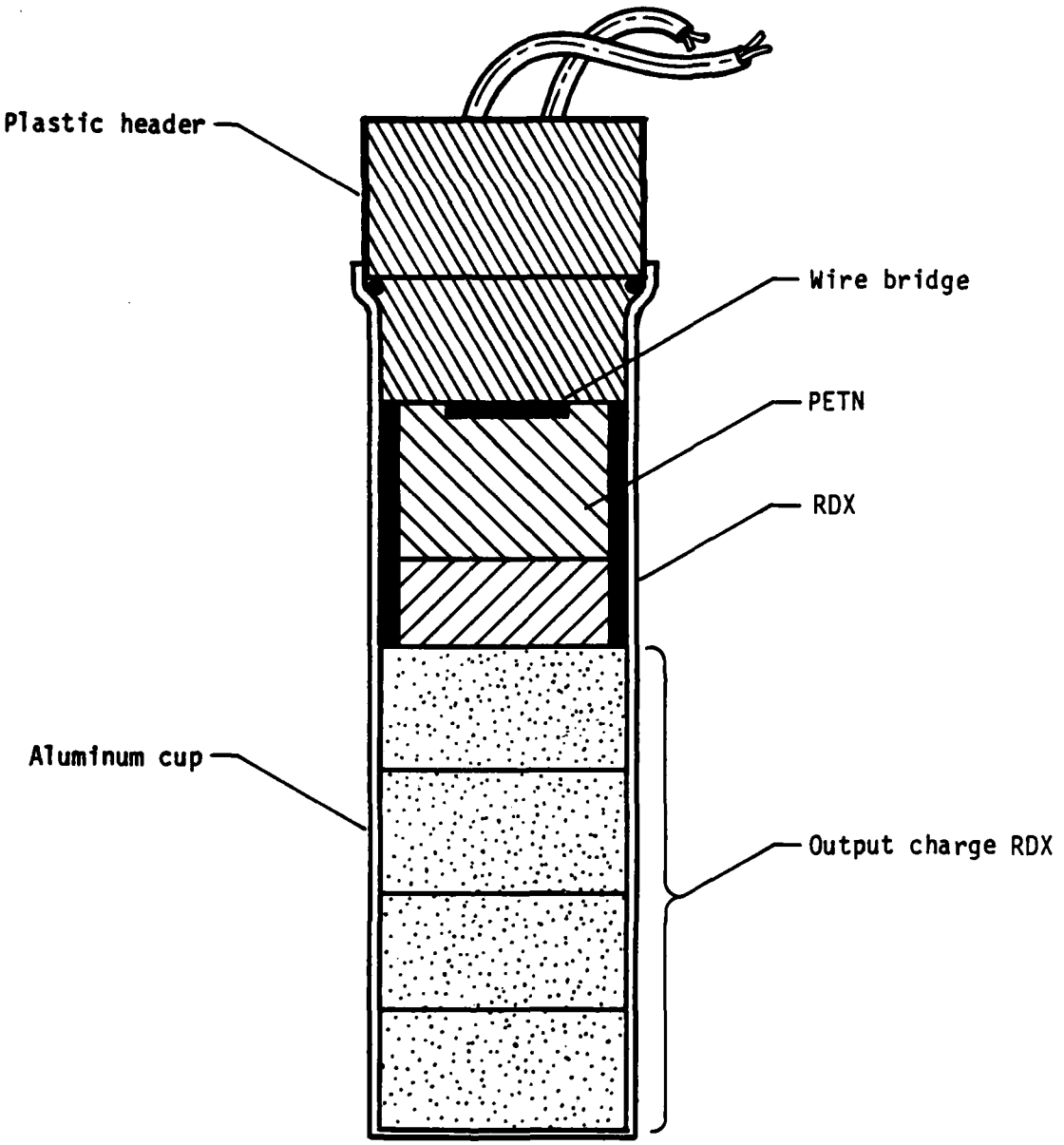

Figure 3. Reynolds Industries RP-83 Detonator.

consists of four individual RDX pressings each weighing 0.220 grams. A review of these features indicated that if the length of the aluminum cup could be altered by the manufacturer, then model charges having the following characteristics might be readily obtained:

Description	Std.	Mod. 1	Mod. 2	Mod. 3
Mass, gram	0.880	0.660	0.440	0.220
Height, inch	0.700	0.525	0.350	0.175
Diameter, inch	0.275	0.275	0.275	0.275
Case Thickness, inch	0.005	0.005	0.005	0.005

The 0.880-gram detonator is the standard RP-83 detonator and it required only an alteration of case thickness (Table 4). Subsequent discussions with the engineering staff of Reynolds Industries led to a contract to have 60 detonators (15 of each) fabricated for use on this project, at an average cost of $11.63 each, approximately $2.20 above the cost of the standard RP-83. Figure 4 is a photograph of these detonators. An additional consideration in the selection of the RP-83 was the safety feature of the exploding wire bridge (EWB). The EWB is virtually insensitive to low voltage and it will not detonate without the application of a high voltage; thus it could not be accidentally exploded.

A review of the scaled weights for the weapons listed in Table 3 and the weights of the model charges indicates several possibilities for exact mass simulations of the weapons listed. For example, the yield of a 250-pound weapon could be simulated by

0.220-gram at 76.25 G
0.440-gram at 60.53 G
0.660-gram at 52.89 G
0.880-gram at 48.06 G

Likewise, the yield of a 1000-pound weapon could be simulated by

0.440-gram at 98.58 G
0.660-gram at 86.13 G
0.880-gram at 78.26 G

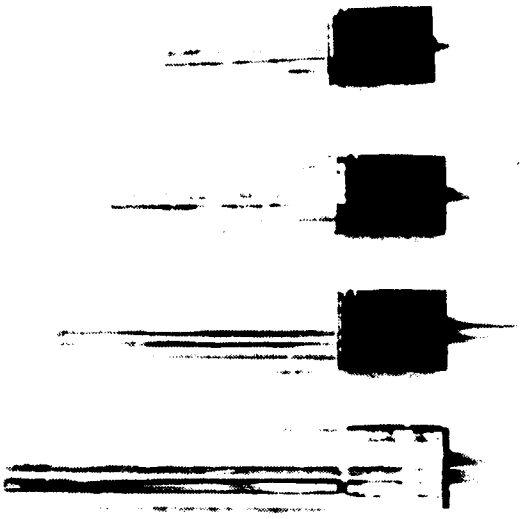

Units are in inches.

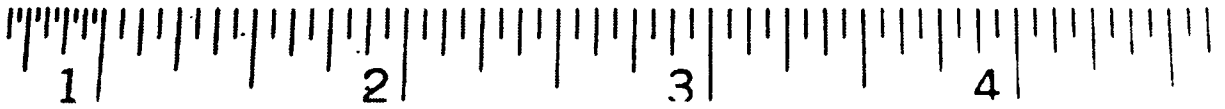

Figure 4. Standard RP-83 and Modified Detonators.

However, in respect to characteristic lengths some violation of similitude had to be tolerated. For example, a review of Table 4 indicates a need for case thicknesses ranging from 0.003 to 0.006 inch. Manufacturing processes limit the case thickness to a minimum value of 0.005 inch. This standard value was selected to minimize costs. This consideration was also influenced by the need to have similitude in the intensive properties of the case materials between the prototype and model. The former values were essentially unknown. Furthermore, this level of detail was considered a tertiary consideration in view of the fact that both the prototype and model configurations stipulated that the weapon would be embedded in the concrete burster slab. Accordingly, it was reasoned that the confining effect of the burster slab would influence the free-field blast parameters more significantly than case thickness.

The diameter of the model charges was a uniform 0.250 inch. This offers a more serious violation of similitude as indicated in Table 4 where an average value of 0.16 inch would appear more appropriate. The effects of this demarcation are not fully known. It is believed that the effect on the recorded peak normal stress is insignificant, perhaps affecting attenuation as reflected in the duration of the positive phase of the pressure pulse. Model charge heights were also standard, being multiples of 0.175 inch. Standard heights and diameter were necessary for economic reasons; alterations to the standard 0.250-inch diameter by 0.175-inch high pressing were cost prohibitive. Numerically, the violation in similitude in respect to height is less severe than that for diametrical simulation. The effect of a height violation was initially judged to be one of loading the burster slab to alter the shape of the wave front in the sand continuum. Subsequent analysis of the data confirmed this judgement. This is discussed in detail in Section IV.

The model charges (Reynolds detonators) were epoxied in place in the model burster slab as indicated in Figure 5. The detonators were epoxied in place to simulate the condition of the prototype weapon; that is, the real weapon does not fully penetrate the burster slab. Under this condition it was assumed that the real weapon would firmly lodge in the burster slab prior to detonation. The use of epoxy to bind the model charge (detonator) to the smooth wall of the model burster slab was an attempt to simulate the real weapon firmly lodged in the real burster slab. The epoxy operation was performed by the ordnance technician after the technician took charge as test conductor, that is, after the test fixture containing the burster slab and

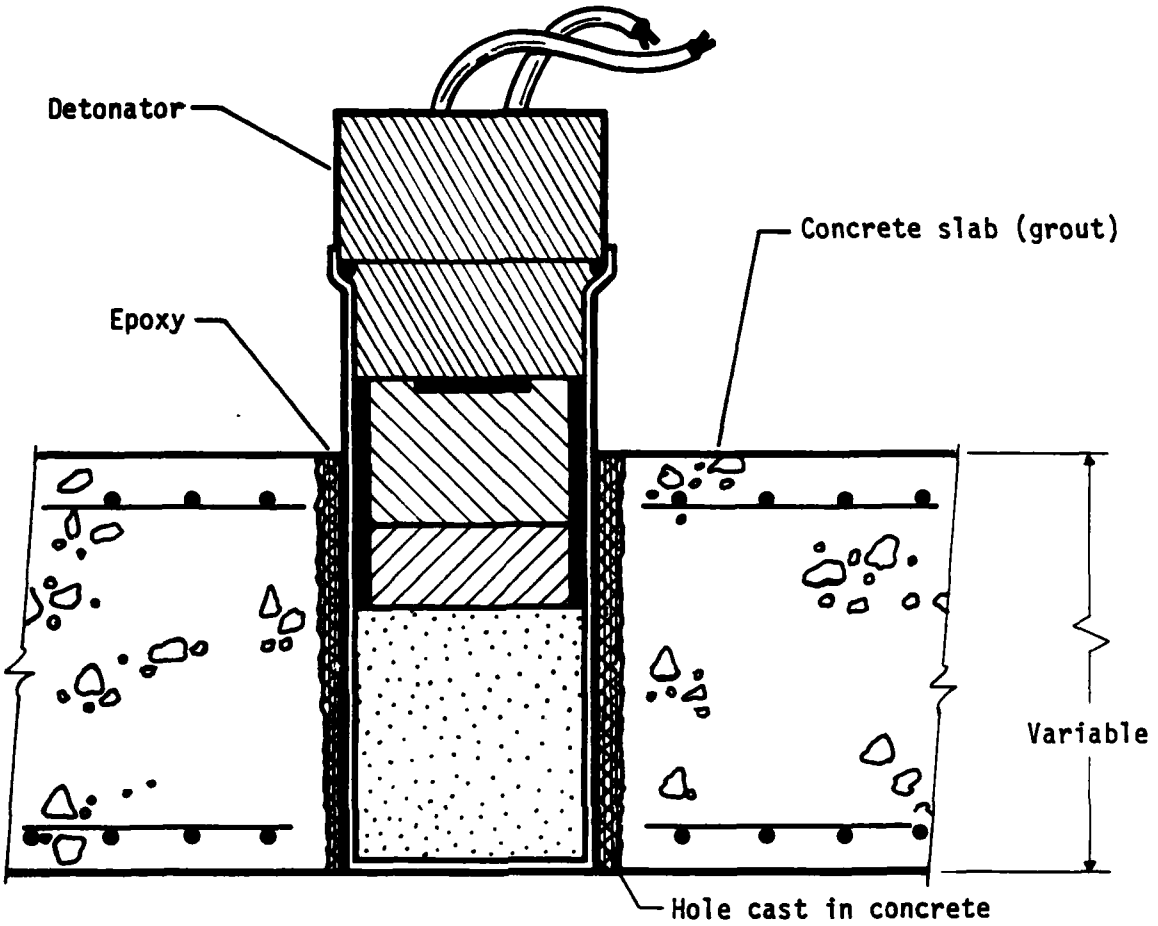

Figure 5. Placement of Detonator in Burster Slab.

sand was attached to the swing-bucket platform on the centrifuge. After the epoxy was set, and with the centrifuge rotating at the prescribed angular velocity, the charge was detonated. A Reynolds Industries Model FS-10 control panel and firing module were used to initiate the EWB within the detonator (model charge). The control panel was mounted externally to the centrifuge, while the firing module was mounted atop the vertical axis of the centrifuge. Voltage was applied to the firing module via a coaxial cable and a slipring, both of which were physically isolated from the data acquisition cables and sliprings. The capacitor discharge firing module produced 3000 volts d.c. However, even with the physical separation of this system from the data acquisition system, both systems were not fully isolated. Thus the high frequency associated with the capacity discharge of the FS-10 was recorded on the data channels.

EXPERIMENTAL PROGRAM

Equation (1) is rewritten here for ease of discussion.

$$\frac{\sigma}{P_0} = F\left[\zeta\left(\frac{P_0}{E_0}\right)^{1/3}, \frac{P_0}{\rho C^2}, \mu, \frac{C_1}{C_2}, \frac{\zeta_1}{\zeta_2}, \frac{\alpha_1}{\alpha_2}, \frac{G}{C^2}, \left(\frac{E_0}{P_0}\right)^{1/3}, \cdots\right]$$

If Equation (1) is considered to model the blast-induced normal stress, σ, in the centrifuge, that is, if material properties do not vary from test to test and if characteristic lengths are scaled according to the G-level, then for the **centrifuge environment**, Equation (1) becomes

$$\frac{\sigma}{P_0} = F\left[\zeta\left(\frac{P_0}{E_0}\right)^{1/3}, \frac{P_0}{\rho C^2}, G\left(\frac{E_0}{P_0}\right)^{1/3}, \cdots\right]$$

If the same type of explosive is used for all tests, then the dependence on P_0 is eliminated and the energy of the explosive can then be replaced with its mass. Thus a simpler form of Equation (1) becomes

$$\sigma = F\left[\frac{R}{W^{1/3}}, G(W)^{1/3}, \cdots\right]$$

where the characteristic length is replaced with R, the range at which σ is to be experimentally evaluated. The terms that remain in Equation (1) are not nondimensional; that is, they are not true π-terms. This does not invalidate Equation (2); rather, it simply means that the magnitude of each term has been

altered; each remains fundamental to the physical process being modeled. If it is assumed that Equation (1) is complete, it can be written as

$$\sigma = F\left[\frac{R}{W^{1/3}}, G(W)^{1/3}\right] \quad (3)$$

Equation (3) defines a surface in a three-dimensional system as shown in Figure 6, where the G-level is confined to the energy term, $G(W)^{1/3}$. Experimental data for the scaled distance $R(W^{-1/3})$ should not reveal any gravity affects because distance scales as $1/n$ and mass as $1/n^3$. Mathematically, at least, the scaling factors are thus equal for both the numerator and denominator, and cancel each other. The purpose of the experiments was to confirm this observation and to demonstrate that centrifugal blast-induced stress data do scale as indicated by Equation (3).

To demonstrate scalability, 12 experiments were planned as outlined in Table 5. In reviewing Table 5,it is important to note that the normal stress measurements were taken at the same scaled range, but that the gages were not at the same range. For example, consider the series of four tests conducted at 50 G and $\lambda = 2$:

W_m, mg	W_p, lb	R, in
220	3.06	1.47
440	3.86	1.86
660	4.42	2.12
880	4.86	2.33

These data demonstrate the term scalability: adjustment of the G-level to scale the yield to produce scaled distances having the same value, but derived from different explosive weights and radial offsets, R. Radial offsets, standoff distances, were located with respect to the bottom of the explosive charge (see Figure 5).

MODEL CONSIDERATIONS

Modeling of the Burster Slab

For purposes of modeling, the prototype burster slab was considered to be 48 inches thick with No. 4 reinforcing bars (temperature) at 14 inches, center to center, both ways, in both the top and bottom of the slab. Rather than model the slab thickness exactly for each G-level used in the experiments, model slab thicknesses were established as indicated in Table 6.

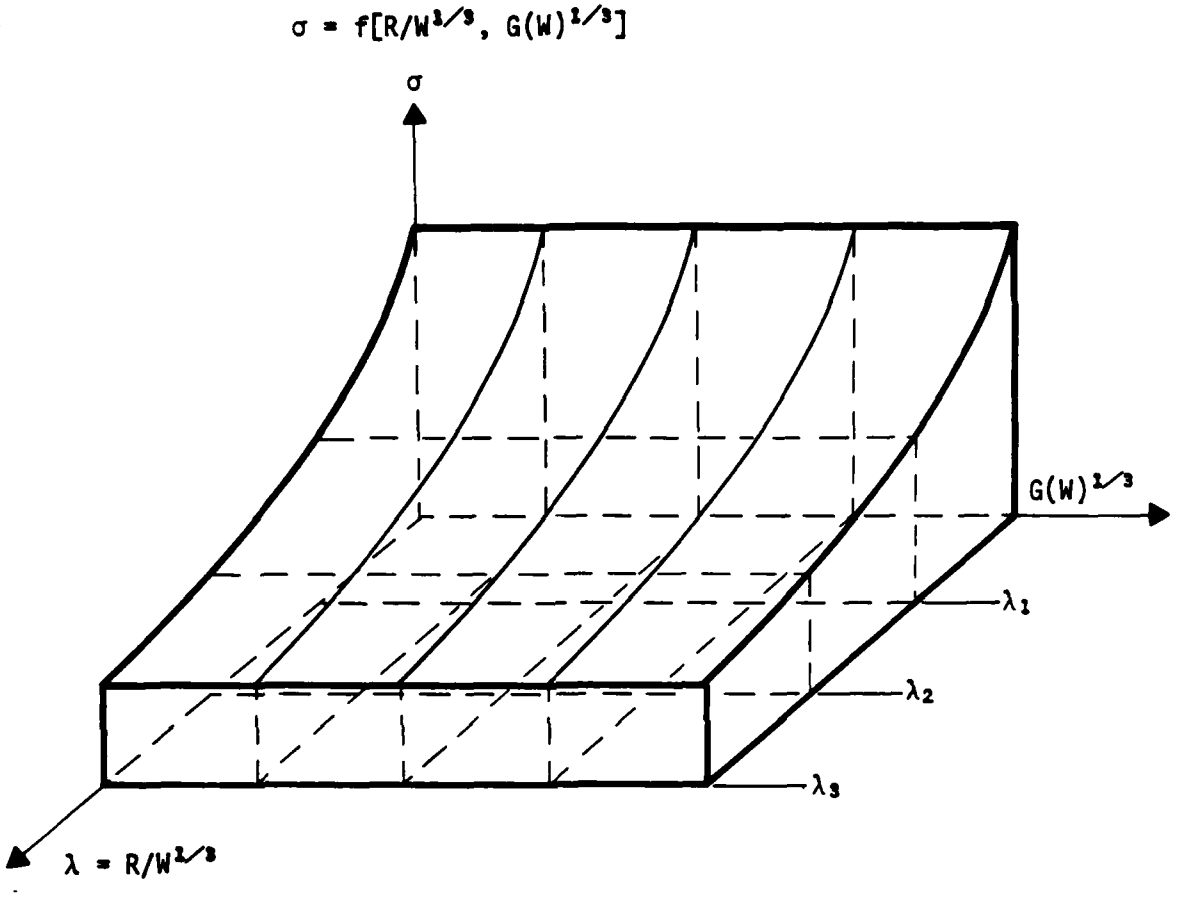

Figure 6. Surface Defined by Equation (3).

TABLE 5. TEST MATRIX.

Explosive weight, mg	G-Level																							
	32			32			40			40			46			[a]50			55			72			79		
	Scaled Distance																									
	λ_1	λ_2	λ_3	λ_1	λ_2	λ_3	λ_1	λ_2	λ_3	λ_1	λ_2	λ_3	λ_1	λ_2	λ_3	λ_1	λ_2	λ_3	λ_1	λ_2	λ_3	λ_1	λ_2	λ_3	λ_1	λ_2	λ_3
880	1	2	3	.5	.8	5	1	2	3	.5	.8	5	--	--	--	.5	1	2	--	--	--	--	--	--	--	--	--
660	--	--	--	--	--	--	--	--	--	--	--	--	.5	.8	5	.5	1	2	--	--	--	--	--	--	--	--	--
440	--	--	--	--	--	--	--	--	--	--	--	--	--	--	--	.5	1	2	--	--	--	--	--	--	--	--	--
220	--	--	--	--	--	--	--	--	--	--	--	--	--	--	--	.5	1	2	1	2	5	.5	.8	5	1	2	--

[a]This series was also conducted in a test series without a burster slab included in the test.

TABLE 6. MODEL BURSTER SLAB THICKNESSES.

G	Simulation Thickness, inches	Selected Thickness, inches
31.44	1.53	1.40
39.60	1.21	1.40
46.37	1.04	0.97
50.00	0.96	0.97
53.00	0.91	0.97
71.88	0.67	0.64
79.52	0.60	0.64

The temperature-reinforcing steel was modeled using standard grade hardware cloth made of 23-gage wire. The hardware cloth has four meshes per linear inch and is commercially available, but only on special order. In respect to simulation, it accurately models the prototype steel percentage at a scale factor corresponding to 50 G, the median of the G-levels reached in these experiments.

The concrete was simulated using a laboratory-developed grout. Laboratory trial mixes included determination of unit weights and 7-day compressive strengths. The selected mix had the properties listed in Table 7.

Circular burster-slabs 21 inches in diameter were cast from mixes having the proportions stated in Table 7. Test cylinders were also cast from each mix. Each model slab was encased in plastic for a cure period of 3 days before removal from its circular steel form. It was then placed in a moist room and cured for at least 28 days before being used in a centrifugal test. Figure 7 is a postshot view of a model burster slab. The wires extending from the slab on each side of the crater were cast into each slab to facilitate the handling of the slab.

TABLE 7. PROPERTIES OF THE MODEL BURSTER SLAB SIMULATED CONCRETE MIX.

Cement, Type I	1.0
Water-Cement Ratio	0.6
Sand	2.33
Baroid	1.0
Plasticizer	0.03
Unit Weight	147 lb/ft^3
Compressive Strength, 28-days	3300 lb/in^2

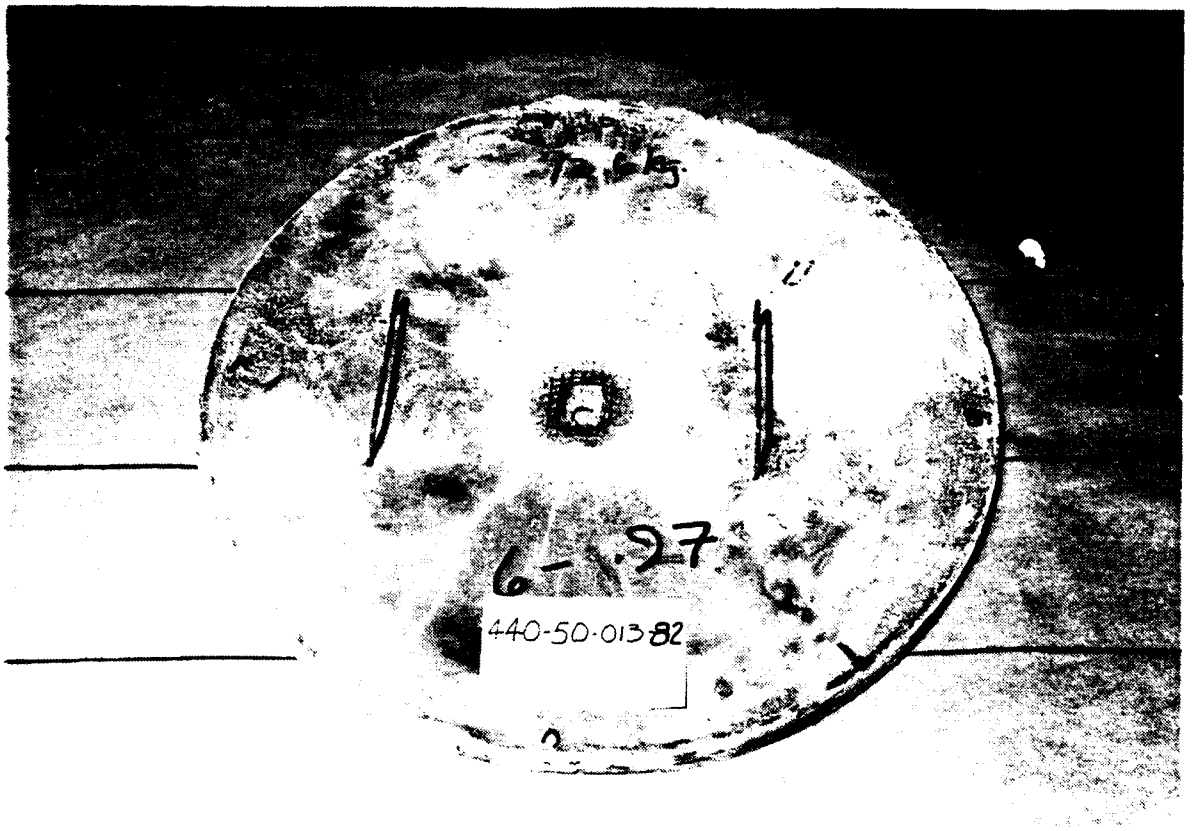

Figure 7. Postshot Condition of Model Burster Slab--440 mg at 50 G.

Modeling of the Sand Continuum

As indicated in the introduction to this section, the burster slab is supported by a sand continuum. No specifications were provided detailing the engineering properties of the prototype sand, other than to assume it to be a quality sand such as that used in a portland cement concrete mix. Such a material would have a gradation ranging from the No. 4 to No. 200 sieve as indicated in Figure 8. Application of the scaling relationships suggests that a sand used in the model should have the particle size distribution indicated on the extreme right of Figure 8. At the G-levels attained in this study, a strict application of the scaling relationship indicates a need for a material with a particle size distribution ranging from the No. 200 size to the 1-micron size. Particles within that size range begin to display clay-like behavior, a significant departure from the granular behavior of the prototype system. Additionally, strict application of the concepts of similitude would require a separate gradation for each G-level and, more importantly, consideration of strain-rate affects. This latter consideration is not well understood and the former suggests the expenditure of considerable effort to prepare each gradation. Because of these considerations it was decided to use a commercially available, fine-grained, well-graded sand; its gradation is also shown on Figure 8. This sand scales the prototype material in the 10- to 15-G range. It was used in all the tests, regardless of the G-level.

Crystal Silica No. 70 sand has the following engineering properties:

Specific Gravity	2.65
Relative Density ASTM D-2049	
Minimum	74 lb/ft^3
Maximum	94 lb/ft^3
Angularity (Reference 7)	Angular

A primary consideration for support of the test program was related to the consistent production of uniform sand models. The customary technique of raining sand into the test fixture was attempted, but this procedure failed to produce models having a consistently uniform density. The raining technique apparently failed because the sand was very fine grain. Several other techniques were attempted without satisfying the placement criterion. A vibration procedure was finally adopted.

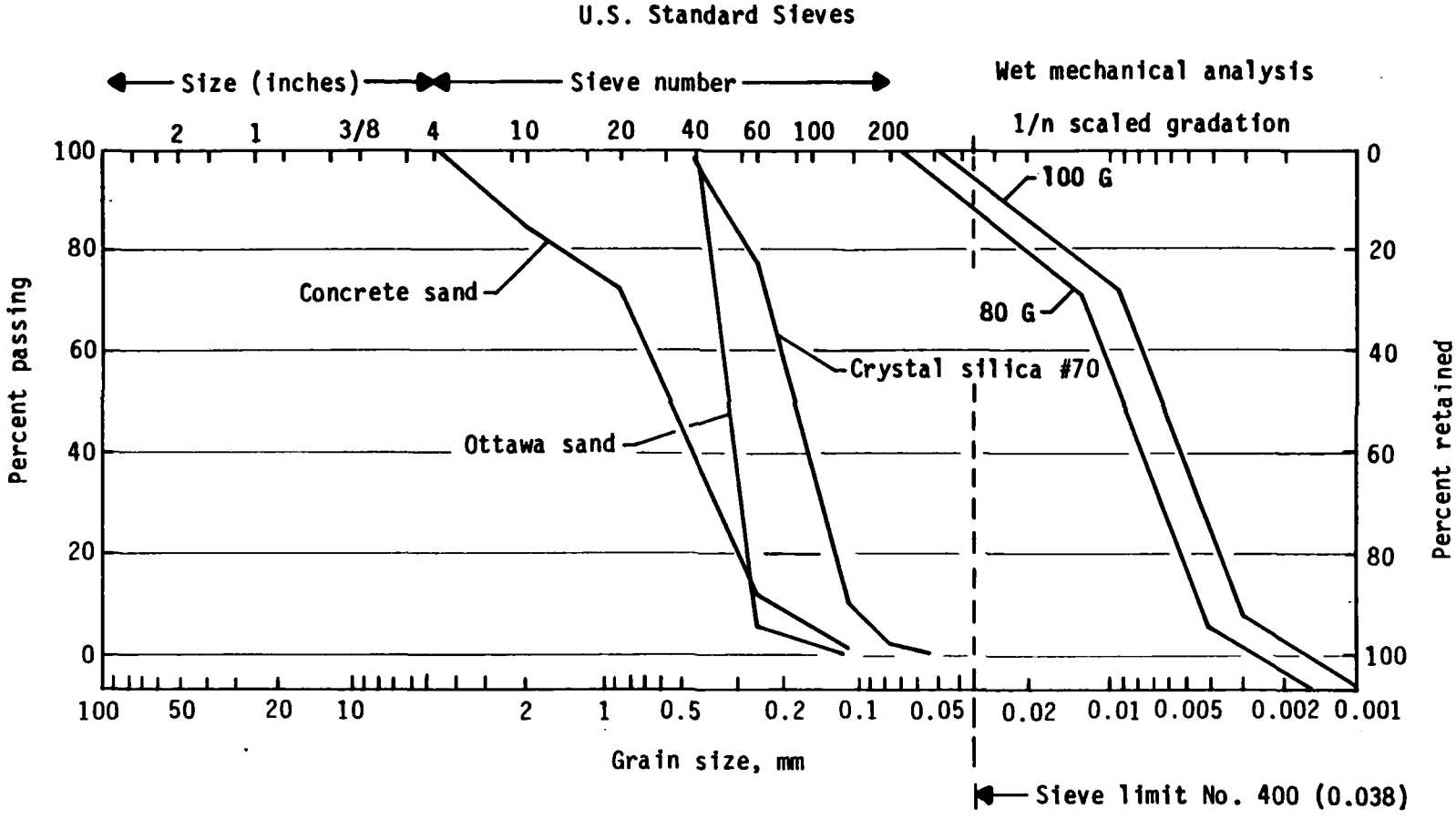

Figure 8. Grain Size Distribution Graph.

Two Airoviber vibrators were rigidly attached to the base of the test fixture (Figure 9). These air-driven vibrators produce 800 pounds of centrifugal force each, when subject to compressed air at 80-lb/in^2 gage. The sand was loosely placed in the fixture in 2-inch layers and vibrated for 10 minutes. This procedure was repeated until the sand was 10 inches deep in the fixture. Actual sand densities were based upon gross weight and the volume occupied by the sand. The mean density for all tests was 103.9 lb/ft^3, the range 101.9 to 105.9 lb/ft^3, the standard deviation 0.80 lb/ft^3, and the coefficient of variation 7 percent.

DATA ACQUISITION

Stress Gage Development

Normal stresses within the sand, generated by the explosion of the model charge, were measured using a foil pressure sensor. Dynasen's carbon-foil pressure sensors, C300-50-EKRTE, were used in this study.* These sensors were selected primarily for size considerations, having nominal dimensions of 0.050 by 0.060 by 0.0025 inch. At the maximum G-level of the centrifuge these dimensions scale to 5 by 6 inches, small enough to represent a point measurement in the prototype field. However, all of the experiments were performed at G-levels below this value; thus the prototype measurement area was smaller, perhaps on the order of 4 square inches on the average. An exploded and enlarged view of the Dynasen pressure sensor is shown as Figure 10.

By necessity these sensors had to be attached to a mounting medium in order to place the sensor in the sand continuum. Having no prior experience with these sensors in a free-field application, several sensor mounting techniques were tried before a successful gage was developed. Thus the initial tests served as a gage-development program. Only several acceptable data records were obtained from these tests because of such problems as debonding, frequency response, debris impact, and strain effects. The gage that eventually evolved consisted of the carbon-foil pressure sensor bonded to 0.008-inch stainless shim stock, cut from sheet rather than rolled shim stock. The shim

*Dynasen, Inc, 20 Dean Arnold Place, Goleta, California 93017.

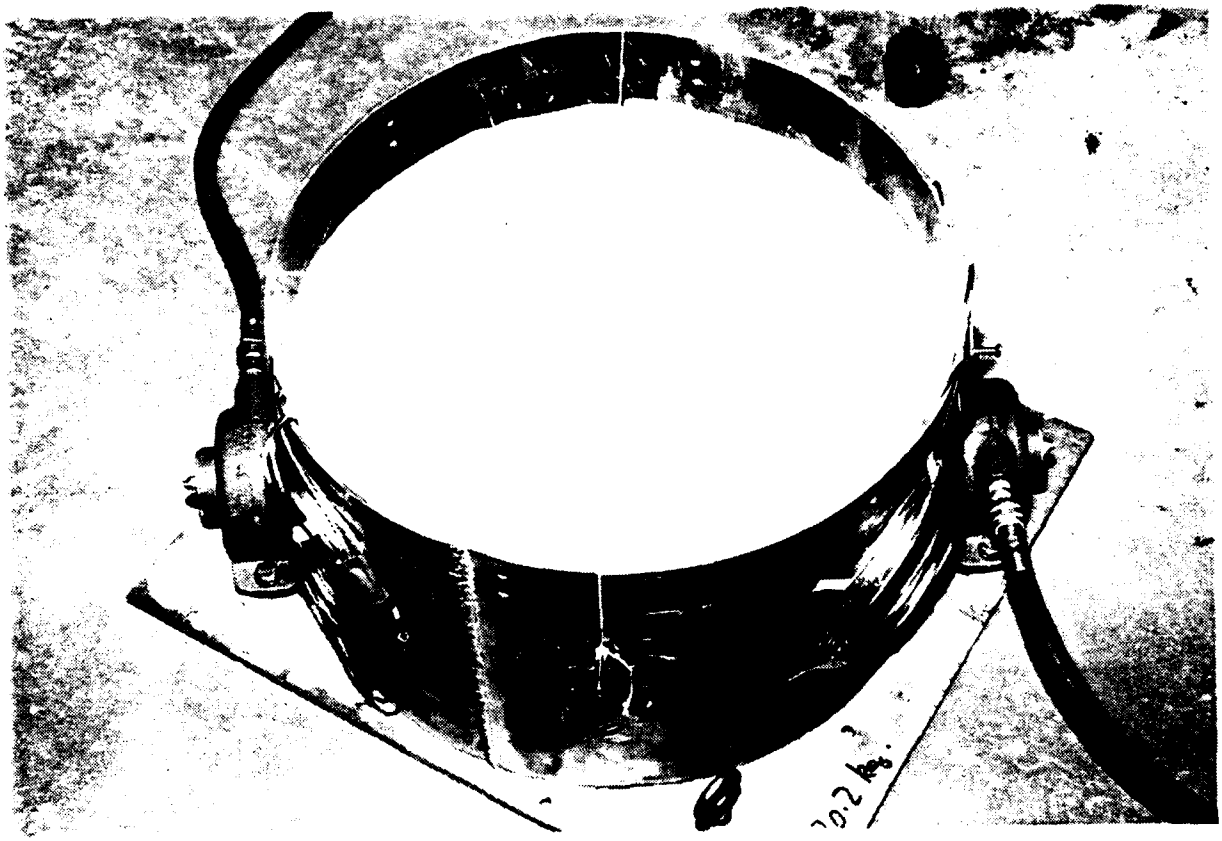

Figure 9. Test Fixture with Vibrators Attached.

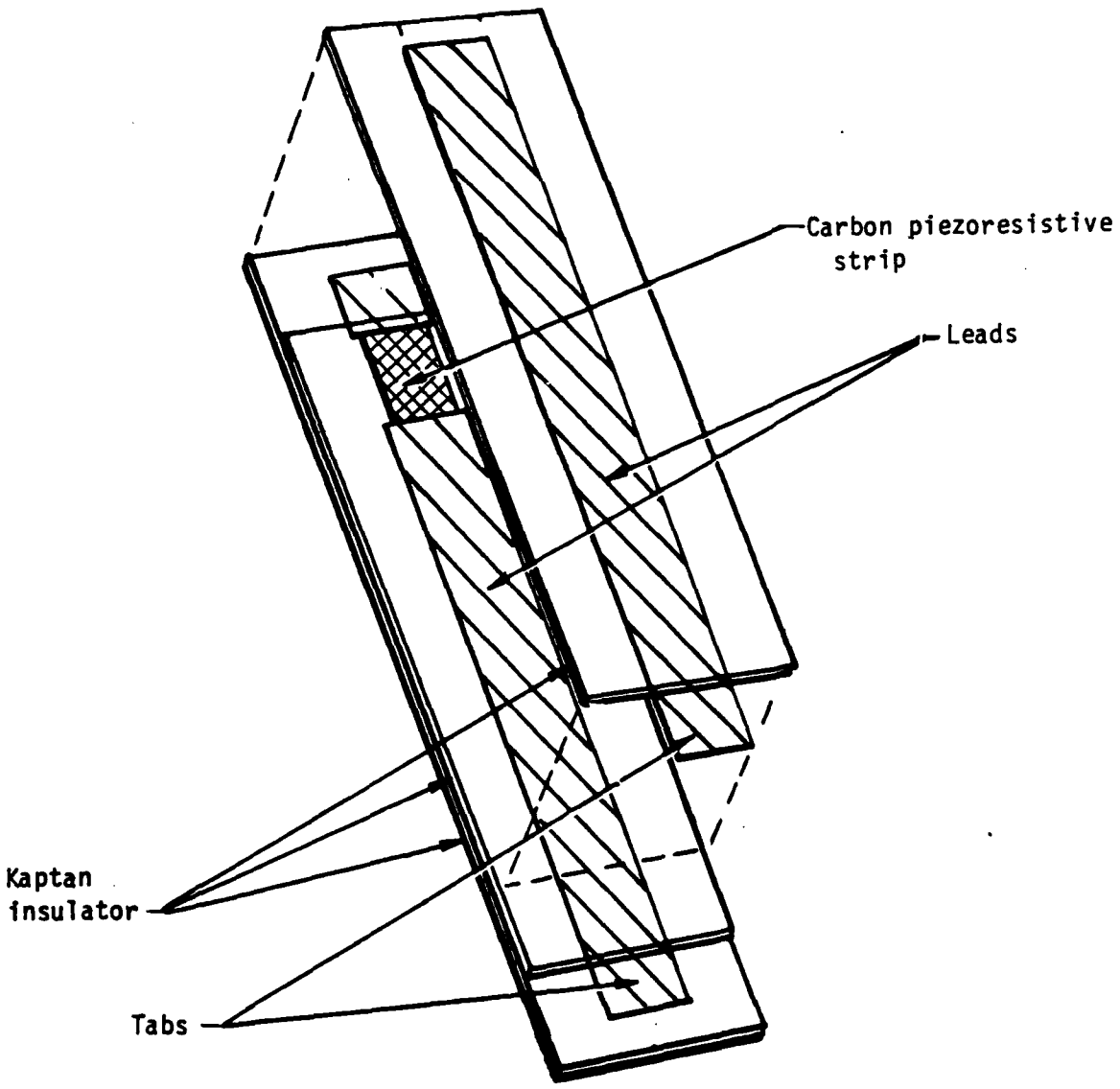

Figure 10. Dynasen's FC300-50-EK Pressure Sensor.

stock measured nominally 2.5 inches long by 0.5 inch wide. The length was necessary to accommodate the 2-inch foil tabs which were attached to the carbon-foil sensor. The sensor and its tabs were bonded to the shim stock with EPY-150. The tabs of the pressure sensor were connected to a 4-wire 1122 Alpha, forming the pressure gage shown in Figure 11. These gages were precisely placed in the sand continuum as suggested in Figure 11.

Instrumentation System

A major problem with the centrifuge cabling system, as it existed prior to this study, was that the 28 data channels were made from single-conductor coaxial cables with unshielded terminals. Pretest evaluation indicated the performance of the system to be poor. It was characterized by excessive cross-talk and a variable frequency response (depending on the termination resistance) with a maximum frequency response of 10 MHz. To improve the response of this system, six of the data cables were replaced with Belden-type, 18-gage, twisted-pair cable, each having a maximum length of 40 feet. Based upon experience with systems of similar characteristics, the frequency response of the upgraded system was estimated to exceed the maximum frequency of interest (240 MHz). However, it was impossible to shield the slip-rings as well as the data cables on the boom of the centrifuge. These deficiencies led to fire-set noise on the data traces and made some records difficult to interpret.

Figure 12 is a wiring diagram for the stress gages. Figure 13 is a block flow diagram of the instrumentation system. All data, including calibration and fiducial, were recorded on standard wide band FM440. Playback was on a Nicolet digital oscilloscope with a hard copy from an x-y recorder.

STRESS GAGE PERFORMANCE

Eighty-two pressure time histories were obtained from the series of tests which included a burster slab. These records were examined for determination of peak normal stress, rise time, stress duration, and time of arrival. This included records obtained during the early phase of the testing program which was essentially a gage-development phase. All of the data were not considered valid because of mechanical failure of the gage, noise on the record, or malfunction of the explosive. Thirty of the 82 data points were considered to be invalid. Figure 14 is a pictorial representation of the observed responses of

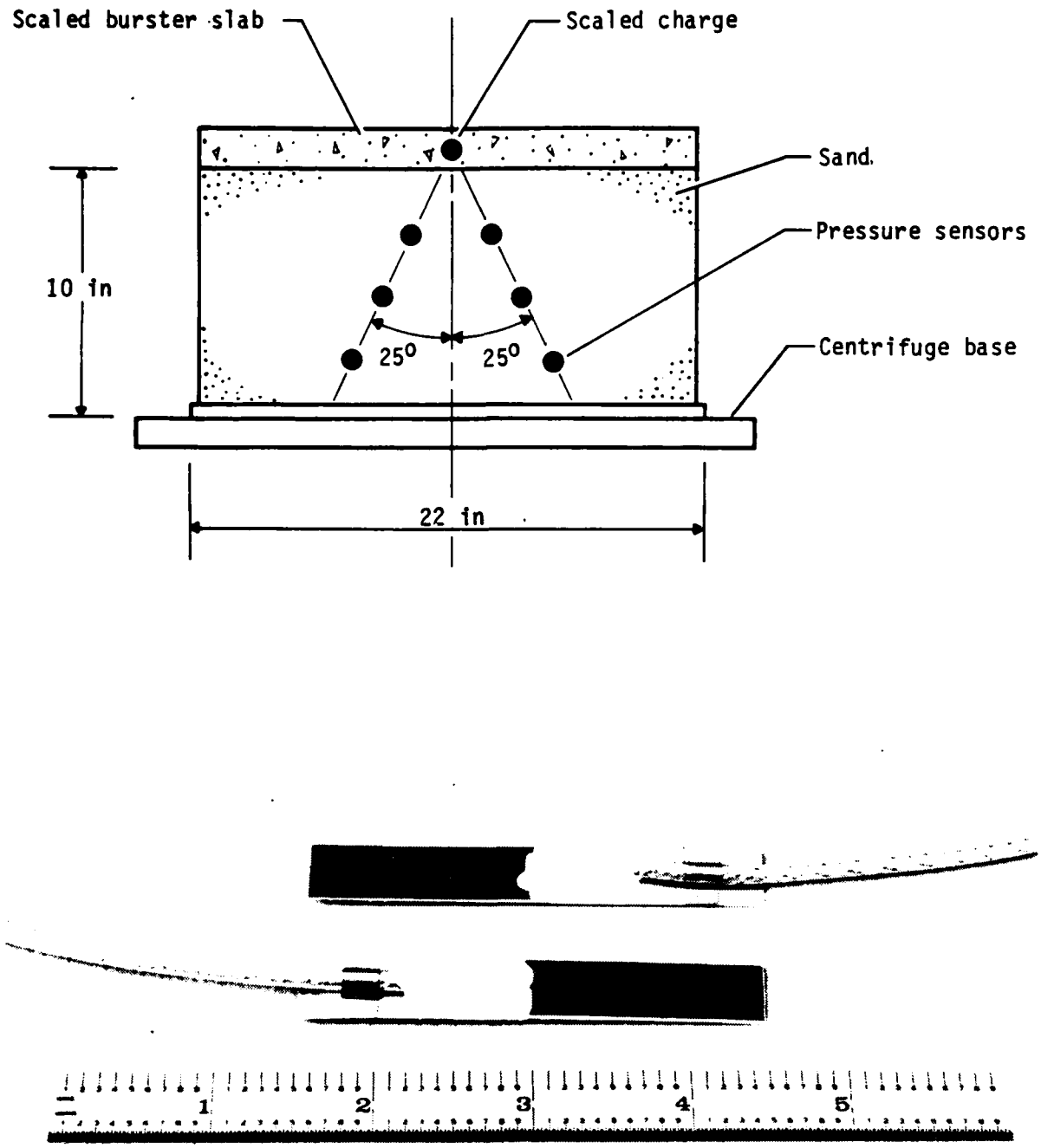

Units are in inches.

Figure 11. Stress Gage and Gage Layout.

R_1 Dynasen shock pressure gage
R_2,R_3 49.9Ω,1 % br. compl. resistor
R_4 100Ω, 10-turn, balance control
R_5,R_6 10 mΩ, amplifier reference
B_1 Battery, 1.5V
B_2 Battery, 24V, cal. relay power
K_1 Calibration relay
SW_1 Calibration control switch
A_1 Dynamics, Mod. 7525, amplifier
D_1 Diode, suppression

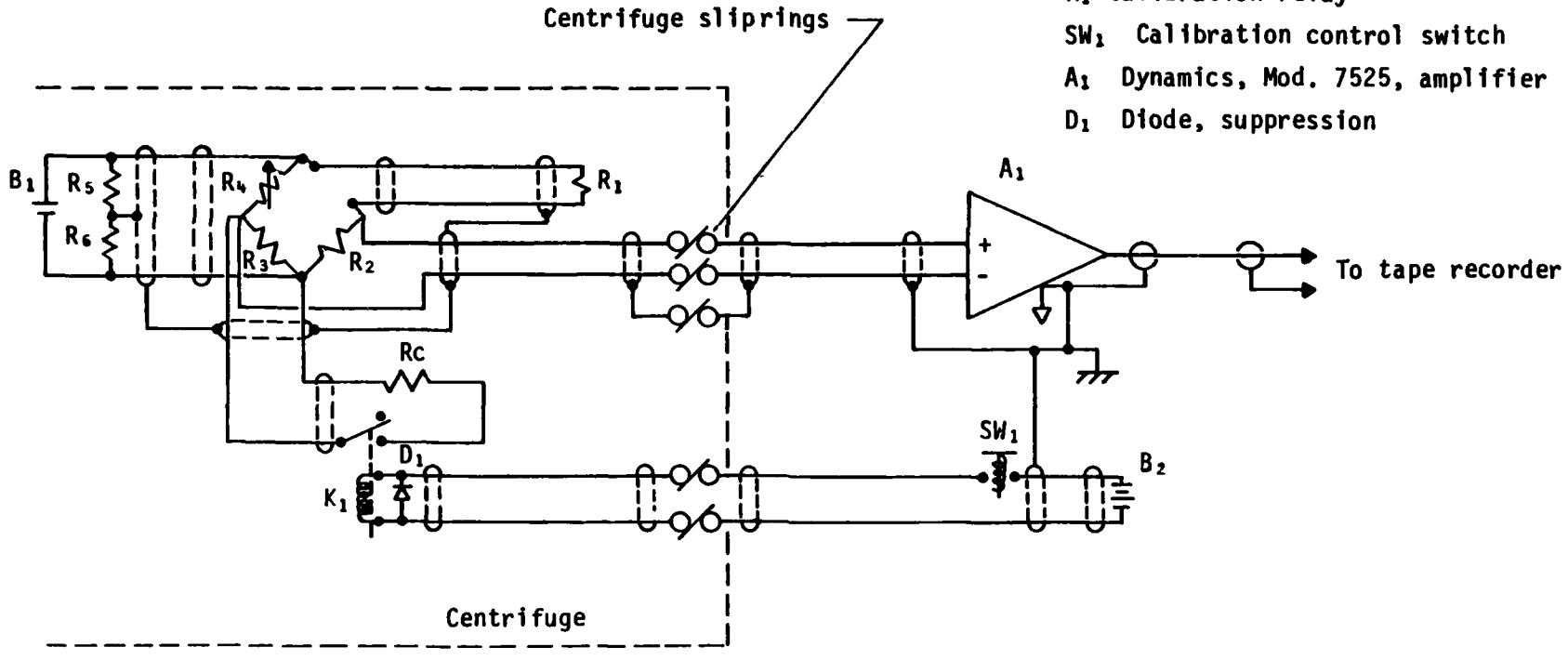

Figure 12. Configuration Detail--Dynasen Shock Pressure Gage.

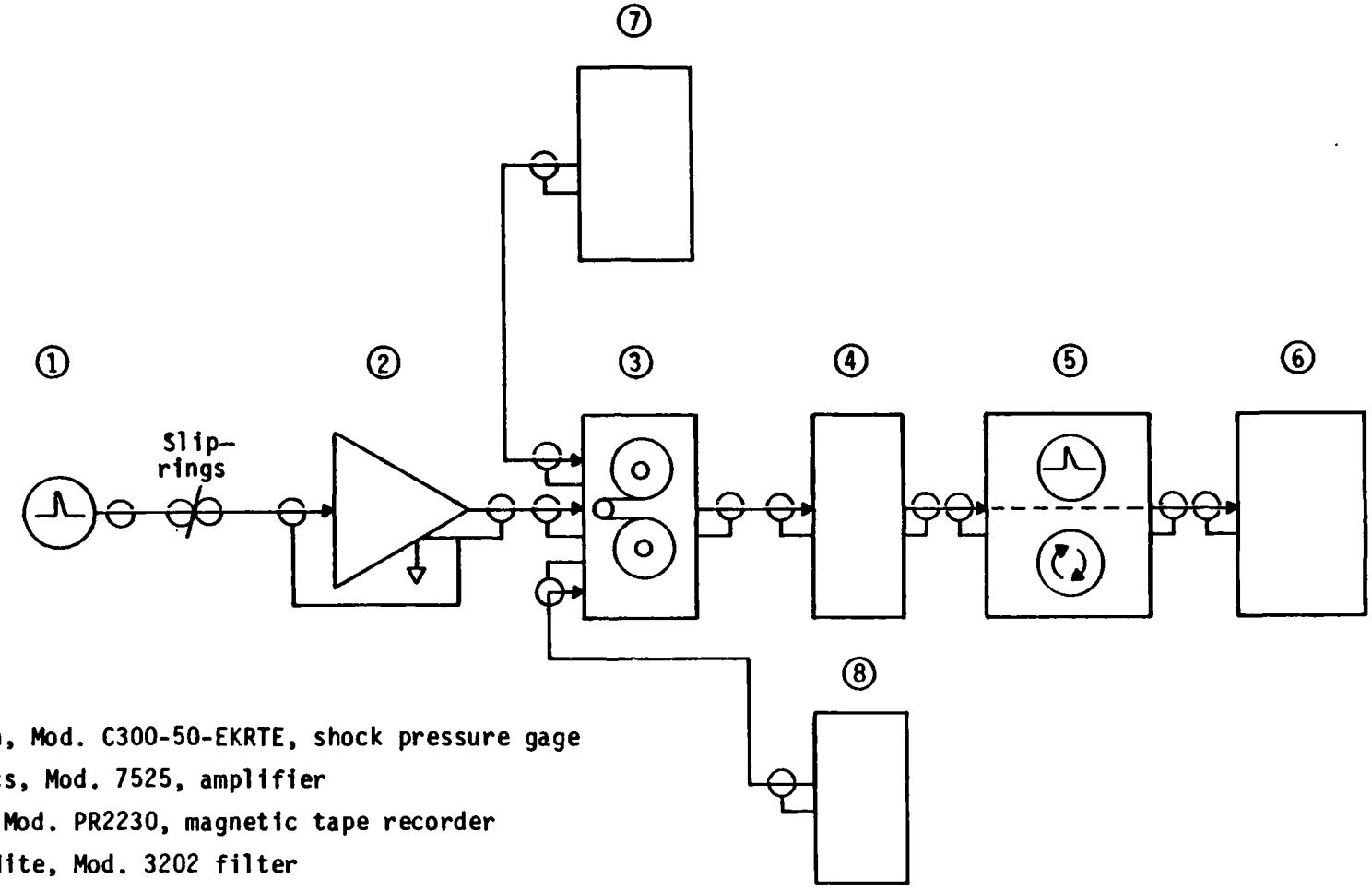

1 Dynasen, Mod. C300-50-EKRTE, shock pressure gage
2 Dynamics, Mod. 7525, amplifier
3 Ampex, Mod. PR2230, magnetic tape recorder
4 Krohn-Hite, Mod. 3202 filter
5 Nicolet, Mod. 204-A, digital oscilloscope, with floppy disk
6 Houston Instruments, Mod. 2000, X-Y recorder
7 Datum, Mod. 9300, time code generator (IRIG B, Mod.)
8 Reynolds, Mod. FS-10, explosives fire control unit (fiducial marker)

Figure 13. Signal Flow Block Diagram--Centrifuge Data Acquisition System.

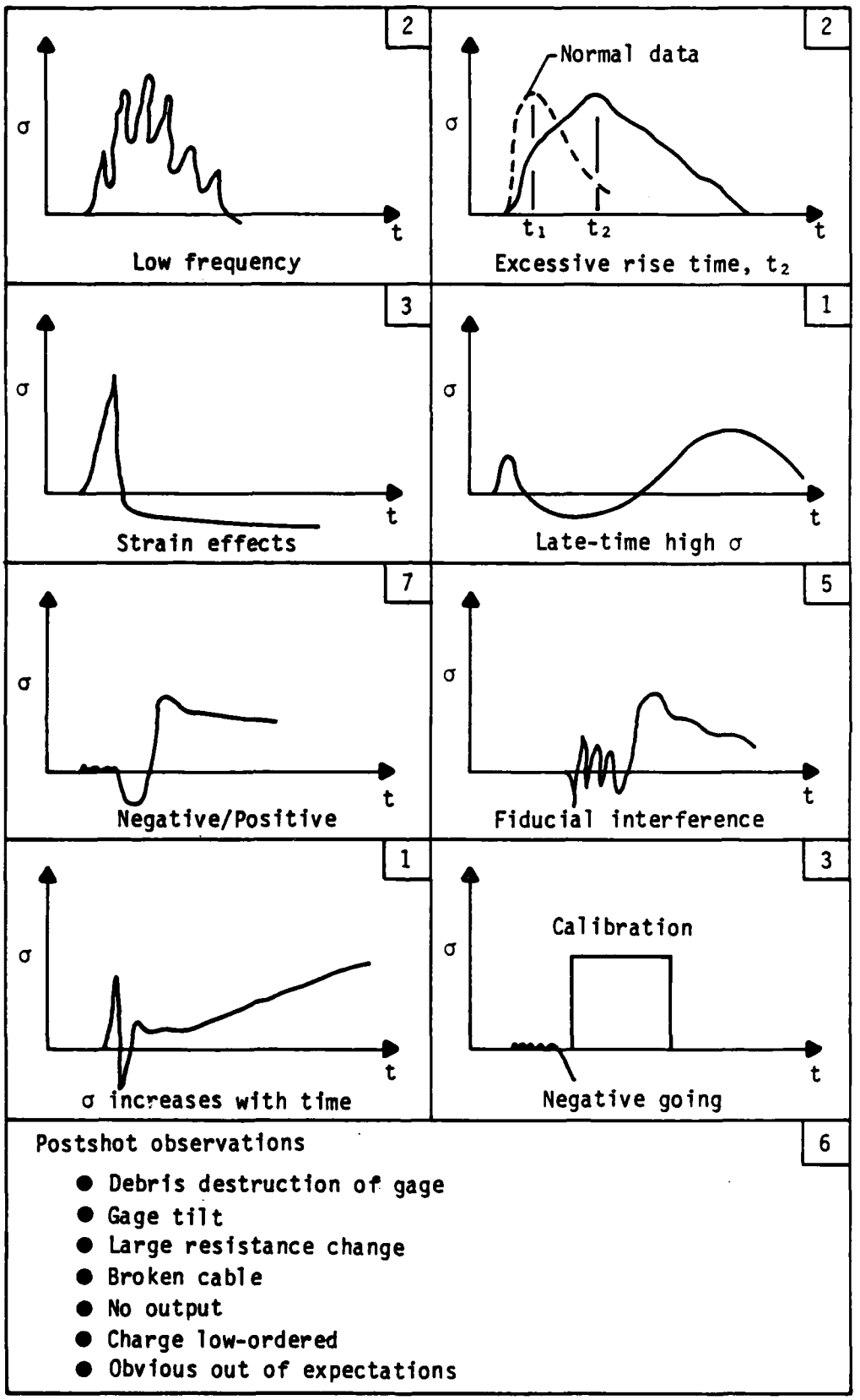

Figure 14. Data Rejection Modes.

the gage which were considered to be unacceptable. The numeral in the upper corner of each frame reflects the number of data traces rejected for the reason indicated. Thirteen records from the first three tests (all repeats of the 660-mg at 50 G) were rejected, principally because of strain effects and broken gages. The other 17 rejected records were scattered uniformly throughout the remaining 11 tests. Seven of these 17 records were rejected because of debonding, the negative/positive rejection mode.

Twenty-three pressure gages were used in the test series conducted without a burster slab; all of these records were considered acceptable.

Figures 15 and 16 are selected normal stress/time records obtained in this study.

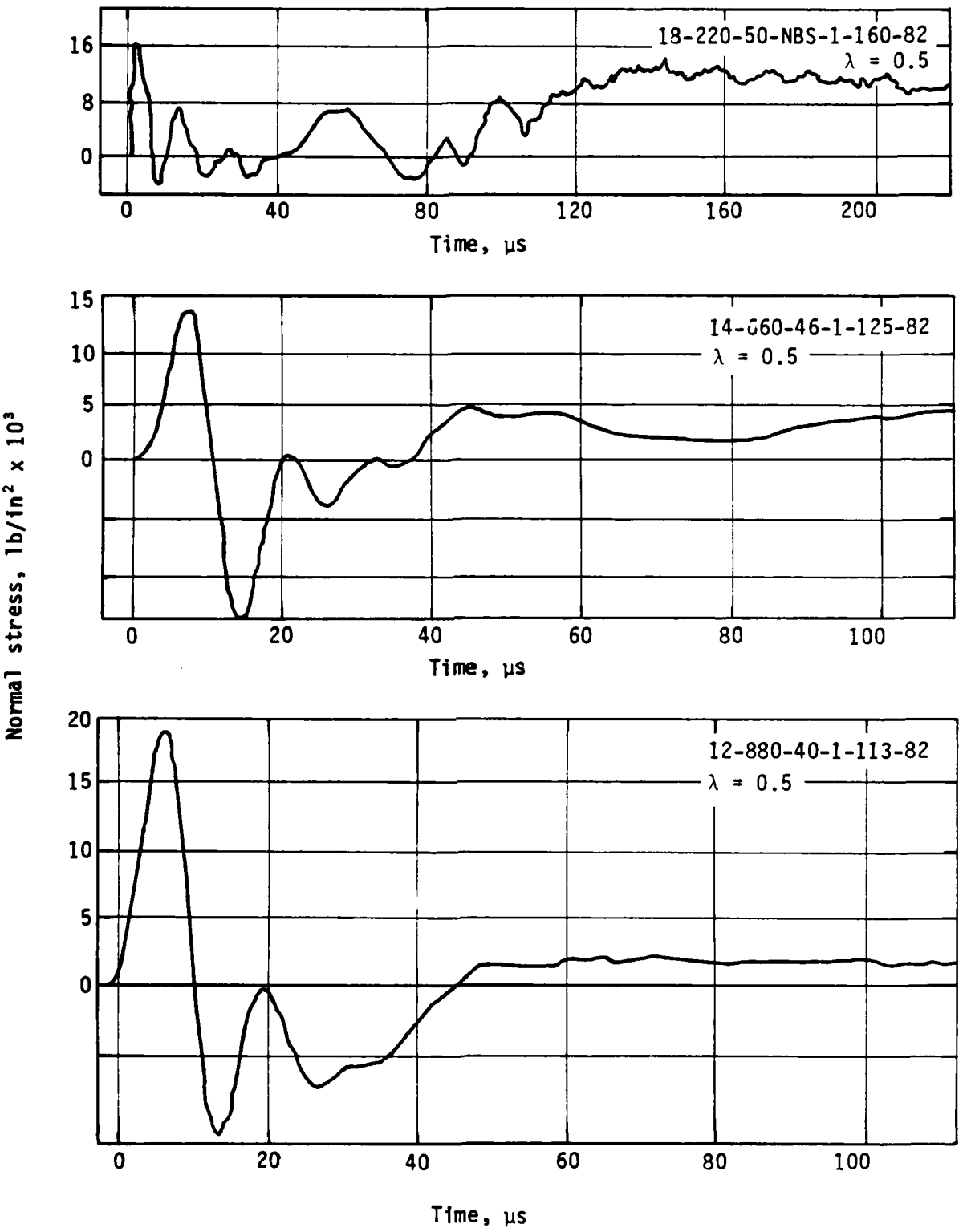

Figure 15. Selected Stress/Time Traces, $\lambda = 0.5$.

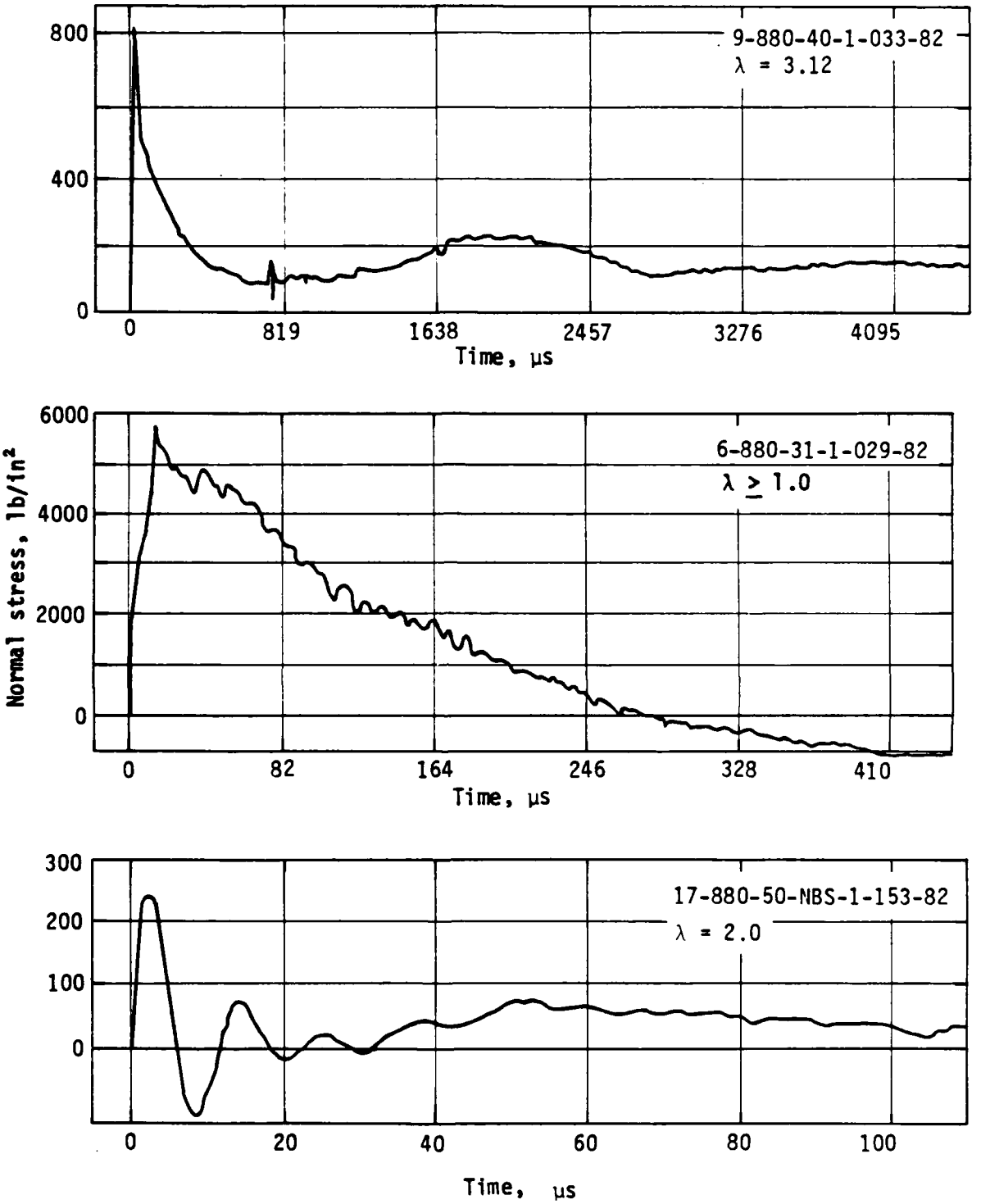

Figure 16. Selected Stress/Time Traces.

(The reverse of this page is blank.)

SECTION IV
RESULTS

TESTS WITH A BURSTER SLAB

Table 8 is a summary of the data obtained from those tests in which a burster slab was included in the test configuration. These data include 52 recordings of normal stress, σ, taken at scaled distances, λ, ranging from 0.5 to 5. The units are lb/in^2 and $ft/W^{1/3}$ respectively. The data also include the sand dilatational wave velocity, C_2 (ft/s). This is a calculated result based upon the known gage location, R, and a determination of the time of arrival of the stress wave at each gage. These data were plotted on normal probability graph paper to determine whether the distribution follows the pattern of a normal curve. These plots are presented as Figures 17, 18, and 19. Rather than plotting the dependent variable, σ, these data are presented in the nondimensional form $\sigma/\rho_2 C_2^2$ which is considered to be a more fundamental term for ground motion studies than σ.

A review of these figures indicates a tendency for the data to plot in a linear manner. This linearity, though subjective, suggests that the data follow the pattern of a normal curve. The implication is that the data contain primarily only random error. In an attempt to control experimental errors, all test models (placement of sand and pressure gages) were prepared by the same technician. In an effort to minimize the effect of improved skills (systematic error), each test (a different combination of model charge weight and G-level) was assigned a test number derived from a random draw.

A review of the normal probability plots indicates an average coefficient of variation of 13 percent for all λ-groups. The range in this statistic is 9 to 20 percent. When examined in terms of normal stress, the data indicate an average variation about the mean of 7 percent at one standard deviation. The average range in normal stress about the mean value is 23 percent. These statistics indicate that the quality control for the experiments was excellent for this type of study, and that the experiments contained a high degree of replication.

TABLE 8. SUMMARY OF TEST DATA FOR TESTS WITH A BURSTER SLAB.

Observation	λ, $ft/lb^{1/3}$	W, mg	G	γ_2, lb/ft^3	C_2, ft/s	σ, lb/in^2
1	0.50	220	85	104.46	1992.8	14560
2	0.50	220	90	104.46	1992.8	12000
3	0.50	440	50	103.75	2050.0	16000
4	0.50	440	50	103.75	1990.0	13870
5	0.50	660	46	105.37	1992.8	13730
6	0.50	880	32	102.43	2070.0	14700
7	0.50	880	32	102.43	2380.0	17700
8	0.50	880	40	103.04	2370.0	18400
9	0.50	880	40	103.04	1992.8	12070
10	0.80	660	46	105.37	1968.0	9720
11	0.80	660	46	105.37	1968.0	8460
12	0.80	880	40	103.04	1930.0	9906
13	0.80	880	40	103.04	1992.8	8104
14	1.00	220	79	104.46	2090.0	6970
15	1.00	220	50	104.56	1992.8	5220
16	1.00	220	50	104.56	2290.0	6970
17	1.00	220	55	105.07	1960.0	6450
18	1.00	220	50	103.75	1992.8	4760
19	1.00	440	50	103.75	2090.0	6120
20	1.00	440	50	103.75	2040.0	6200
21	1.00	660	50	95.42	1992.8	4890
22	1.00	880	50	103.95	2190.0	7170
23	1.00	880	31	103.95	1992.8	5720
24	1.00	880	31	103.85	2160.0	5330
25	1.00	880	40	104.96	1992.8	4930
26	1.00	880	40	104.96	1992.8	4460
27	2.00	220	72	104.46	1992.8	2420
28	2.00	220	55	105.07	1870.0	2200
29	2.00	220	55	105.07	1750.0	2220
30	2.00	220	79	104.46	1992.8	2540
31	2.00	220	50	104.56	2170.0	2020
32	2.00	220	50	104.56	1992.8	2560
33	2.00	220	80	104.46	1992.8	2450
34	2.00	440	50	103.75	1992.8	2100
35	2.00	660	50	95.42	1992.8	2790
36	2.00	660	50	95.42	1992.8	2100
37	2.00	660	50	103.54	1992.8	2850
38	2.00	880	50	103.95	2020.0	1940
39	2.00	880	31	103.85	1700.0	2710
40	2.00	880	40	104.96	1670.0	2300
41	3.05	880	31	103.85	1992.8	1290
42	3.05	880	31	103.85	1992.8	1220
43	3.12	880	40	104.96	1992.8	810
44	4.91	220	50	104.56	1992.8	786
45	4.91	220	50	104.56	1992.8	900
46	4.96	220	55	105.07	1830.0	690
47	5.00	220	72	102.83	2000.0	726
48	5.00	660	46	105.37	1968.0	730
49	5.00	660	46	105.37	1968.0	692
50	5.00	880	40	103.04	1992.8	703
51	5.00	880	40	103.04	2060.0	803
52	5.00	880	32	102.43	1960.0	640

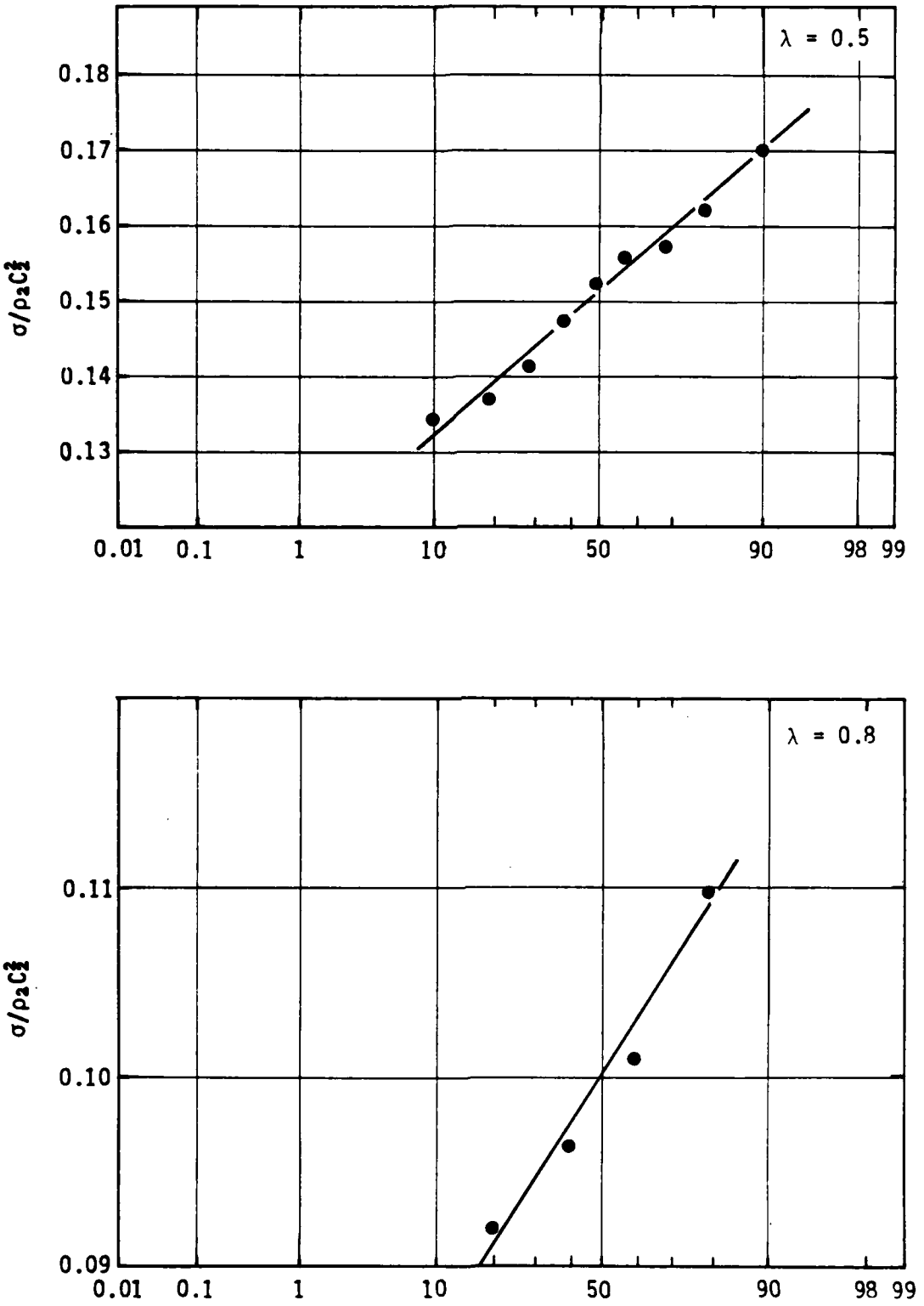

Figure 17. Normal Probability Plot of Nondimensional Stress for Tests with a Burster Slab, λ = 0.5 and 0.8.

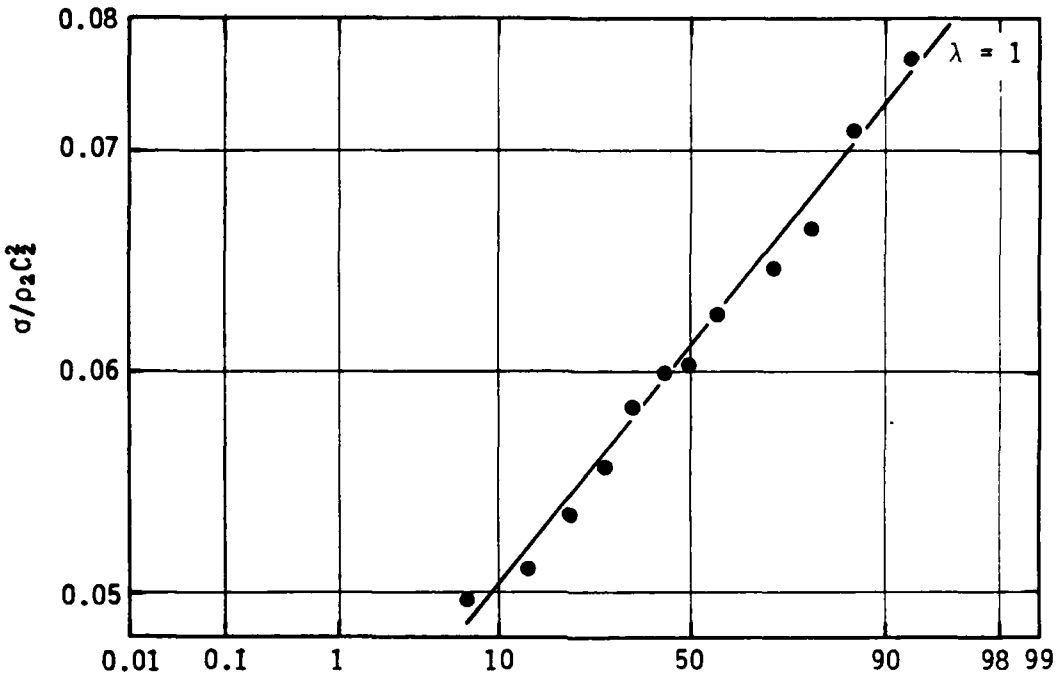

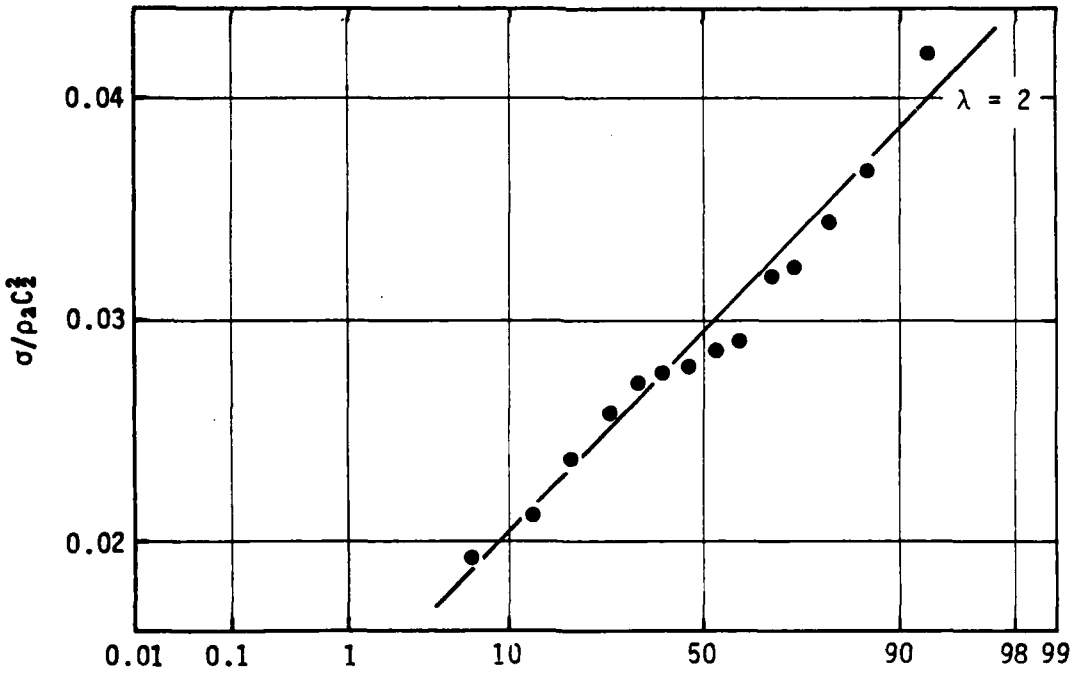

Figure 18. Normal Probability Plot of Nondimensional Stress for Tests with a Burster Slab, λ = 1 and 2.

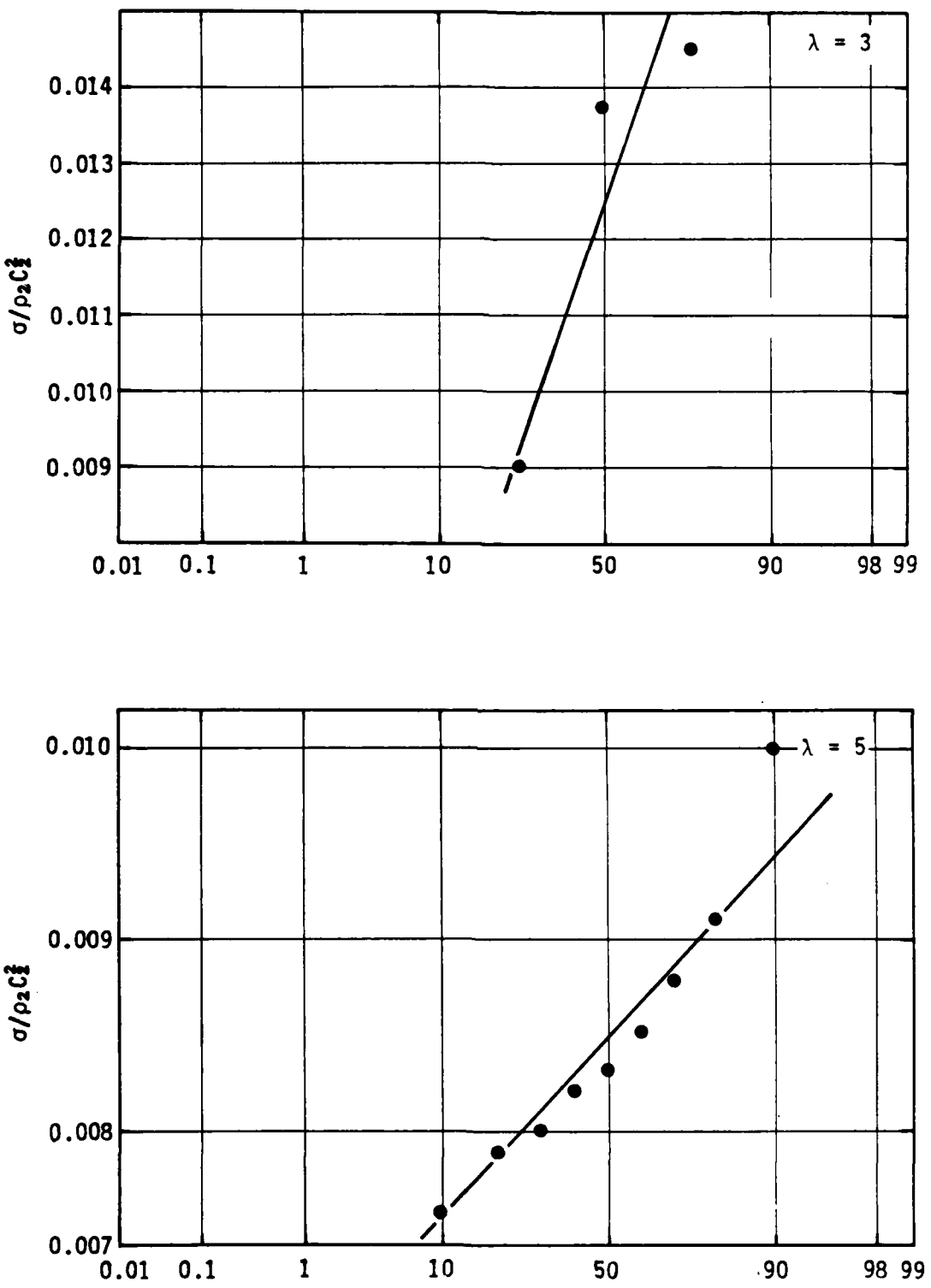

Figure 19. Normal Probability Plot of Nondimensional Stress for Test with a Burster Slab, $\lambda = 3$ and 5.

All sources of error inherent to the experiments are not known. A gage or explosive charge placement error of 0.02 inch (a reasonable expectation) results in an average error of 4 percent in the scaled distance. The close-in gages are more adversely affected by placement errors than those gages at a larger range. However, no statistic could be found that suggests other than a random error with respect to gage or explosive location. Pressure sensor calibration was provided by the manufacturer. Each sensor could not be calibrated because the process is essentially destructive to the sensor. The sensors are manufactured in small batches. Sensors randomly selected from each batch are calibrated. The manufacturer stipulates that the maximum variation for sensors from different batches is 5 percent from the calibration provided and less than 5 percent intrabatch. However, the sensors were mounted on shim stock to form a stress gage. The Civil Engineering Research Facility (CERF) did not, however, have the equipment required to calibrate these gages, so the manufacturer's calibration had to be used.

Probably the largest single source of random error lies in the determination of time of arrival used to compute dilatational velocity, C_2. An error in the determination of the time of arrival on the order of 1 microsecond (a reasonable expectation) results in a variation of the dilatational velocity of nearly 4 percent. This translates into an error in $\sigma/\rho_2 C_2^2$ of more than 8 percent. The accumulation of all of these known sources of error easily exceeds the variation observed in the data. Clearly, the quality control on the experiment was acceptable.

The variable of primary interest in this study is the normal stress, rather than the ratio $\sigma/\rho_2 C_2^2$. The ultimate application is that of predicting σ as a function of the scaled distance, λ. Therefore the paired observations of these variables were subjected to multiple linear regression analyses to determine the functional form of the best-fit relationship between σ and λ. The criterion of least squares was used to provide an estimate of the equation of the regression line. The strength of the fit was evaluated on the basis of the correlation coefficient calculated for each linear relationship obtained from the analysis. This statistic was selected because the data points (σ_i, λ_i) for $i = 1, 2..52$, are values of a pair of random variables. That is, neither variable can be assumed to be known without error,

and thus the data are a sample of a bivariate population. The assumption that the bivariate sample has a normal distribution (the errors are random) is derived from Figures 17, 18, and 19, and the foregoing discussion concerned with experimental errors.

Figure 20 is a plot of the paired values of σ_i, λ_i presented in Table 8. These data are plotted on log-log scales. This transformation permits a linear regression analysis and was necessary because a suitable fit to the data could not be found in the arithmetic domain. A linear relationship is necessary for a least-square fit. Least squares estimators of the true relationship have the smallest variance and are the most reliable in the sense that they are subject to the smallest chance variation. The best single-variable model fit to the data is

$$\sigma = 5879\lambda^{-1.325} \tag{4}$$

where

σ = vertical normal stress, lb/in^2
λ = scaled distance, $ft/lb^{1/3}$

for which the sample correlation coefficient, r^2, has a value of 0.979. This value indicates that 98.9 percent of the sample variation in log σ can be attributed to the linear variation in log λ. By application of the Fisher transformation, the 95-percent confidence interval of $0.982 < r < 0.994$ has been established as an estimate of the true strength of the linear relationship between log σ and log λ. The standard error of estimate in the exponent is 0.027; for the coefficient, it is 0.01017 applied to its logarithm. Equation 4 is plotted on Figure 20. Evidence of the goodness of fit is revealed in Figure 21. This figure is a plot of the residual $(\log \sigma_i - \log \bar{\sigma}_i)$ versus $\log \lambda_i$, where $\bar{\sigma}_i$ is the predicted value of σ_i. The inference that the fit is good is based upon the observation that the residuals appear to be equally distributed about the zero residual.

Other multiple-variable, linear models were developed in an attempt to improve on the correlation coefficient. However, no significant improvement in this statistic was detected. A summary of these models follows.

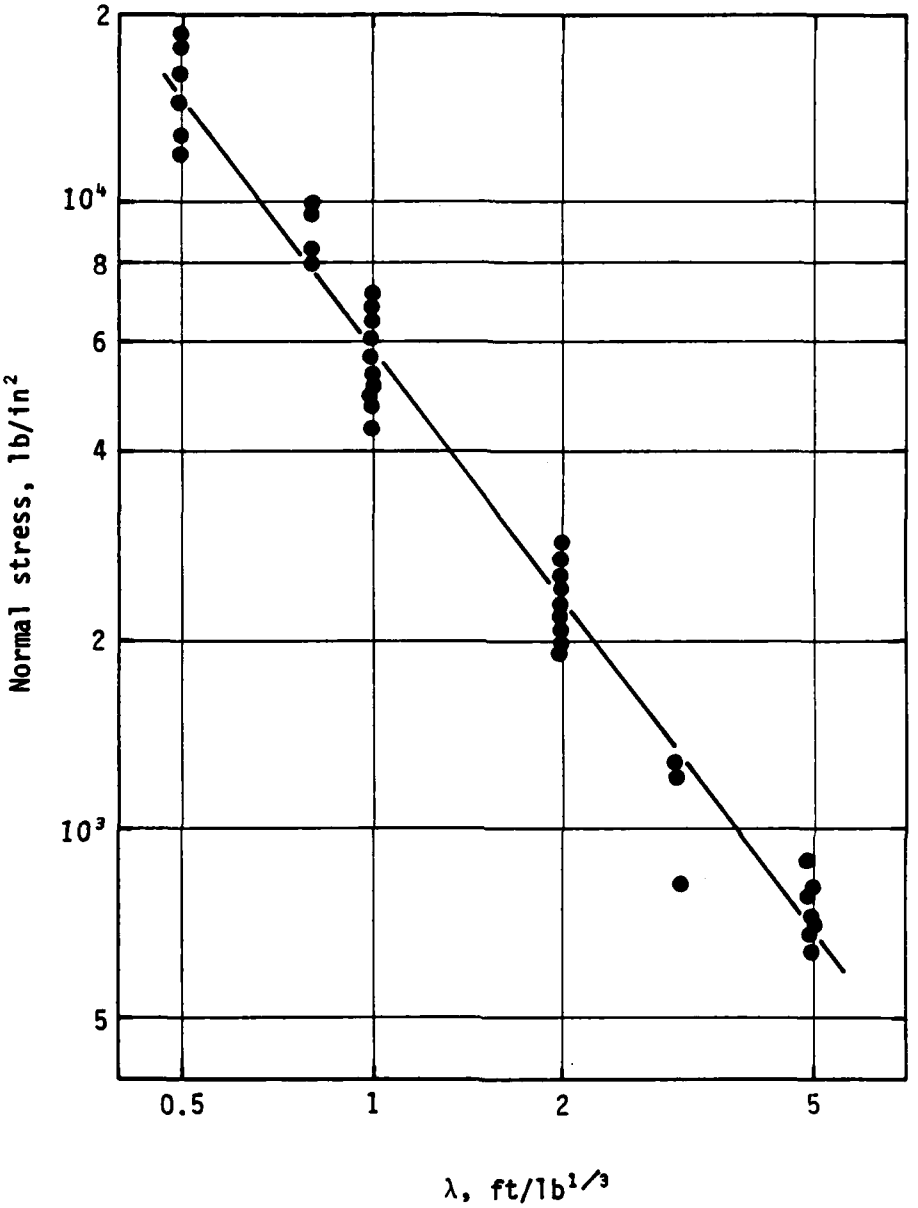

Figure 20. Data for Tests with a Burster Slab.

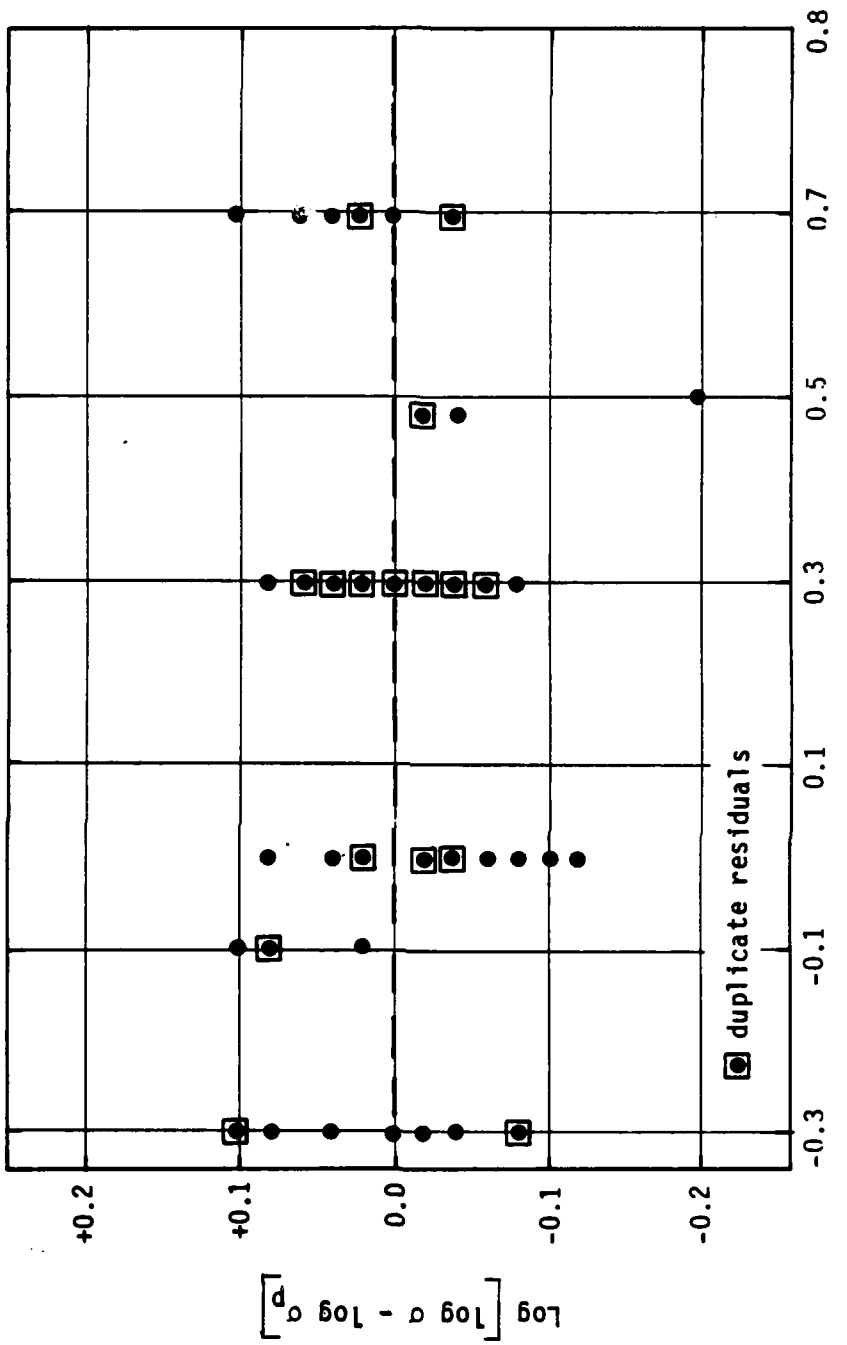

Figure 21. Goodness-of-Fit Plot.

$$\log \sigma = -1.325 \log \lambda + 5.9277 \qquad r^2 = 0.9792$$

σ = normal stress, lb/in^2

λ = scaled distance, $ft/lb^{1/3}$

$$\log \sigma = -1.325 \log \lambda - 0.098 \log \lambda' + 5.9670 \qquad r^2 = 0.9794$$

λ' = scaled depth of burster slab

$$\log \sigma = -1.327 \log \lambda - 0.030 \log \lambda'' + 5.9279 \qquad r^2 = 0.9794$$

λ'' = scaled charge length

$$\log \sigma = -1.324 \log \lambda - 0.101 \log \lambda' - 0.031 \log \lambda'' + 5.9715 \qquad r^2 = 0.9796$$

In reviewing Figure 20 it is important to recognize that the data points at a particular scaled distance contain only a few repeat tests. To the contrary, the ordinate values are derived from tests with explosive yields scaled according to the similitude relationship developed in Section II. The range in data is due to experimental error. None of the forms of the dependent variable (σ_1, σ/P_0, $\sigma/\rho_2 C_2^2$) revealed significant correlation with the G-level; in a regression analysis, the maximum observed value of the correlation coefficient was 0.144. Thus the data in the σ,λ-plane (Figure 20) does not contain any gravity effects. These data were also analyzed to determine if any consistent trends could be observed relative to the weight of the explosive, W_m. The data were grouped according to the weight of the explosive; and then a linear regression was performed to determine the coefficients in the linear relationship between $\sigma/\rho_2 C_2^2$ and λ. This form of the dependent variable was chosen because it contains a larger random error than σ. The results, shown in Table 9, indicate no significant difference between the individual groups and that for the entire group of weights. There is an indication that the attenuation decreases with increasing weight. The effect is not due to weight; it is due to shape of the charge. The shape of the model charge becomes increasingly cylindrical as its weight increases (see Section III).

TABLE 9. SUMMARY OF REGRESSION ANALYSIS TO EVALUATE EFFECT OF MODEL EXPLOSIVE WEIGHT.

W_m	No. of Tests	Equation[a]	r^2
220 mg	18	$\sigma/\rho_2 C_2^2 = 0.389\ \lambda^{-1.219}$	0.980
440 mg	5	$\sigma/\rho_2 C_2^2 = 0.318\ \lambda^{-1.386}$	0.997
660 mg	9	$\sigma/\rho_2 C_2^2 = 0.359\ \lambda^{-1.304}$	0.985
880 mg	20	$\sigma/\rho_2 C_2^2 = 0.360\ \lambda^{-1.292}$	0.958
Combined	52	$\sigma/\rho_2 C_2^2 = 0.357\ \lambda^{-1.271}$	0.970

[a]Feet-slugs-seconds

The other π-term involved in these experiments is $G(W)^{1/3}$. Because W in that term is $(W_m \cdot G^3)$, no gravity effects should be detected in a linear regression analysis with σ as the dependent variable and $G(W)^{1/3}$ as the independent variable, at any value of λ. Thus, because $G(W)^{1/3}$ is an energy term, at $\lambda = 0$ the detonation pressure is independent of the energy and the σ versus $G(W)^{1/3}$ relationship should have a zero slope. Likewise, at any other value of λ, the slope should remain zero, except that the value of σ decreases with increasing λ. The relationship is the surface previously shown in Figure 6.

Linear regression analyses of the data in Table 8 confirmed the shape of the surface. A linear function of the form $\sigma = m[G(W)^{1/3}] + b$, was fit to the data at $\lambda = 0.5$, 1, 2, and 5. In all cases, except $\lambda = 0.5$, the slope values (m) were such that $-0.4 < m < 4$ and the intercept values (b) were in acceptable agreement with the stress predicted by Equation(4)at the corresponding values of λ.

As noted, the results at $\lambda = 0.5$ did not agree with the assumed shape of Figure 6. The best-fit line for $\lambda = 0.5$ had the form $\sigma = -17[G(W)^{1/3}] + 21{,}394$, with a correlation coefficient of 0.44. While this indicates a low correlation, the slope departs significantly from the former values ($-0.4 < m < 4$) and the intercept is nearly 40 percent larger than the value given by Equation(4)at $\lambda = 0.5$. A review of the data for $\lambda = 0.5$ indicates that the

departure from a zero slope is due to an error in the design of the experiment. As it developed, the heavier charges (880 mg) were accelerated to the lowest G-levels, while the smallest (220 mg) were taken to high G-levels. The result is that at low values of $G(W)^{1/3}$ the charges were truly cylindrical, while at high values of $G(W)^{1/3}$ the charge shape was more nearly spherical. Hence, a case of cylindrical divergence versus spherical divergence, or higher stresses close in for the 880 mg charges. A tabulation of selected data clearly shows the trend.

	$G(W)^{1/3}$	W_m
17,700 lb/in^2	306	880 mg
13,730 lb/in^2	400	660 mg
12,000 lb/in^2	482	220 mg

Interestingly, if the data points associated with the 880 mg are removed from the data set at $\lambda = 0.5$, the slope falls into the range reported above ($-0.4 < m < 4$) and the intercept is within 10 percent of that predicted by Equation(4). If all the data are fit to a model, based upon the considerations of cylindrical divergence, both the slope and intercept remain unacceptable, because the smaller charges do not simulate cylindrical shapes. The choice then is to remove the 220 mg data from the set; the fit improves, $m < 7$, and the intercept exceeds the stress given by Equation(4)by 11 percent. The clear conclusion is that at $\lambda < 0.5$ charge shape is an important factor.

TESTS WITHOUT A BURSTER-SLAB

A series of four tests without a burster slab was performed for the primary purpose of investigating the influence of the burster slab on the attenuation of normal vertical stress, σ. This series was planned after the results from the tests having a burster slab indicated less attenuation than predicted. All details in this test series were identical with those tests which included a burster slab. The model charge was placed at a depth in the sand corresponding to the thickness of the burster slab, had it been present.

Because all tests in this series were performed at 50 G the depth of burial was a constant 0.97 inch. The data obtained from this series are presented in Table 10. Radial offsets, standoff distances, were located with respect to the bottom of the explosive charge. Interestingly, 23 gages were used in this series and none of the data was rejected for any of the reasons outlined in Section III. The normal distribution tendency of these data is apparent from a review of Figures 22 and 23. Figure 24 is a plot of these data, vertical stress σ (lb/in^2) versus scaled distance λ ($ft/lb^{1/3}$).

TABLE 10. SUMMARY OF TEST DATA FOR TESTS WITHOUT BURSTER SLAB.

Observation	λ, $ft/lb^{1/3}$	W, mg	G	γ_2, lb/ft^3	σ, lb/in^2
1	0.5	220	50	103.44	20070
2	0.5	220	50	103.44	16880
3	0.5	440	50	105.40	13610
4	0.5	440	50	105.40	11820
5	0.5	660	50	103.54	17130
6	0.5	660	50	103.54	16500
7	0.5	880	50	103.60	14200
8	1.0	220	50	103.44	1690
9	1.0	220	50	103.44	1950
10	1.0	440	50	105.40	1730
11	1.0	440	50	105.40	2070
12	1.0	660	50	103.54	1930
13	1.0	660	50	103.54	2110
14	1.0	880	50	103.60	1840
15	1.0	880	50	103.60	1810
16	2.0	220	50	103.44	375
17	2.0	220	50	103.44	240
18	2.0	440	50	105.40	390
19	2.0	440	50	105.40	453
20	2.0	660	50	103.54	511
21	2.0	660	50	103.54	630
22	2.0	880	50	103.60	305
23	2.0	880	50	103.60	235

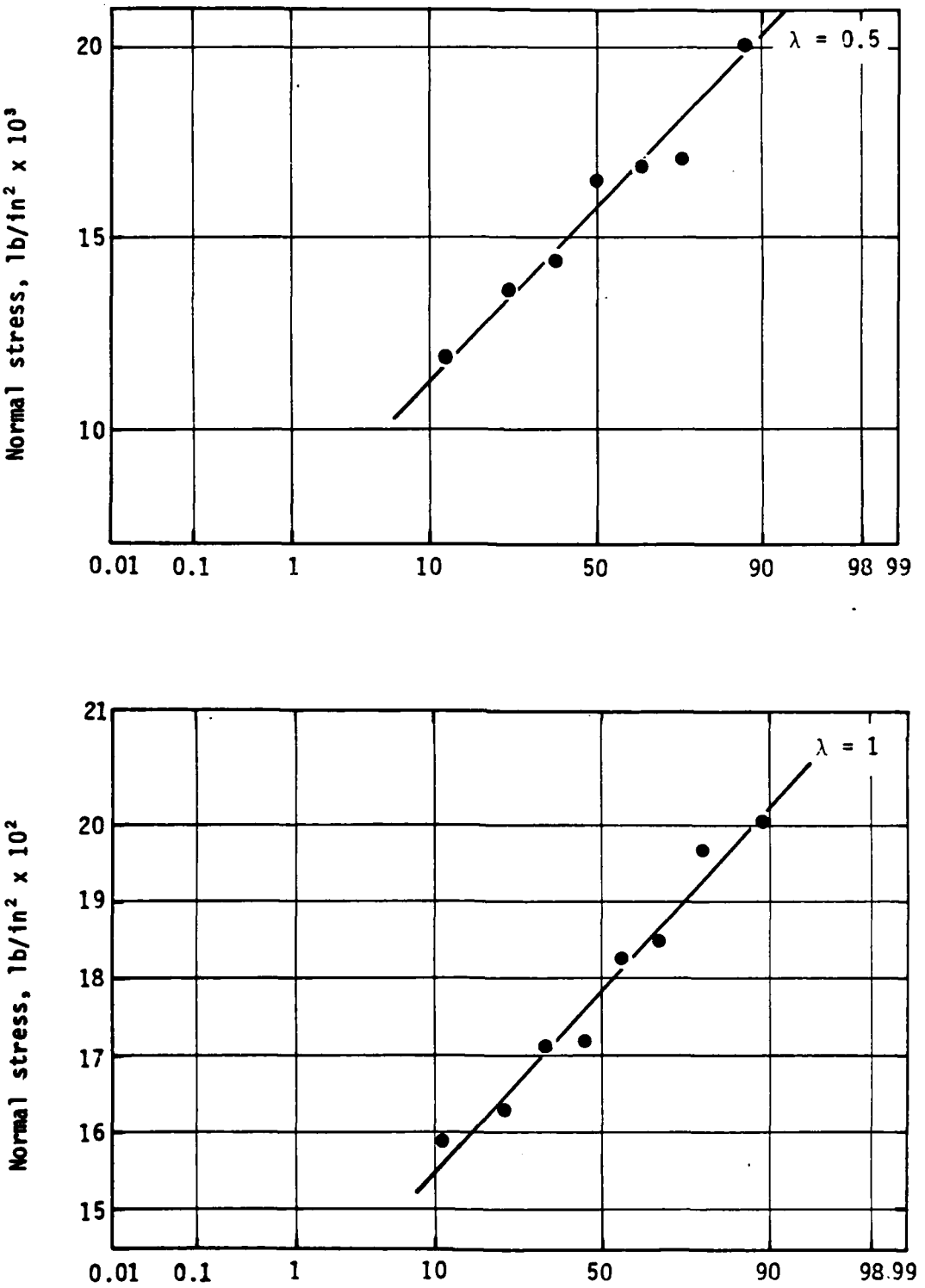

Figure 22. Normality Plot of Normal Stress for Tests Without Burster Slab, λ = 0.5 and 1.

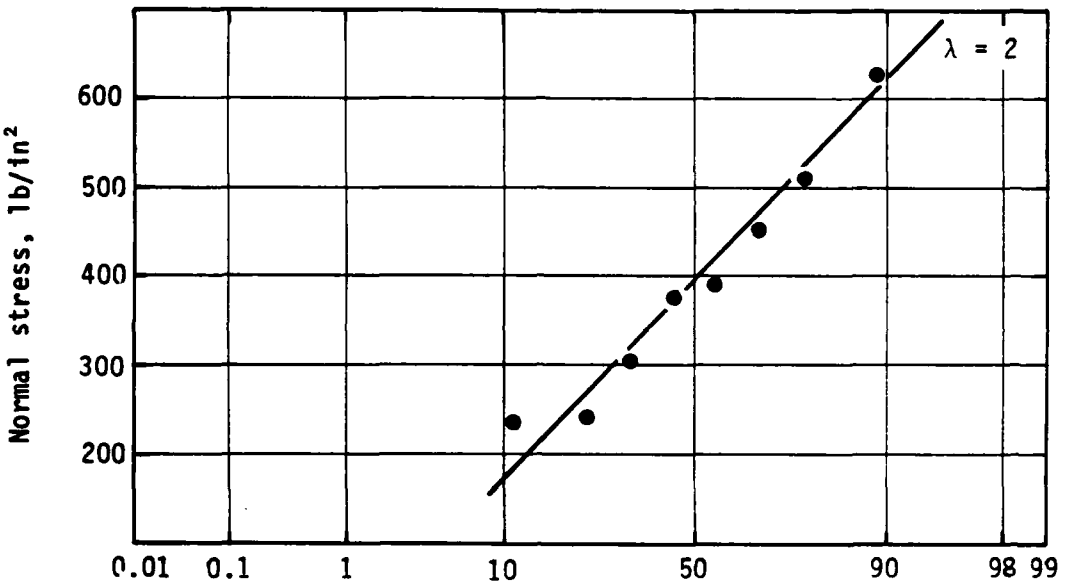

Figure 23. Normality Plot of Normal Stress for Tests Without Burster Slab, $\lambda = 2$.

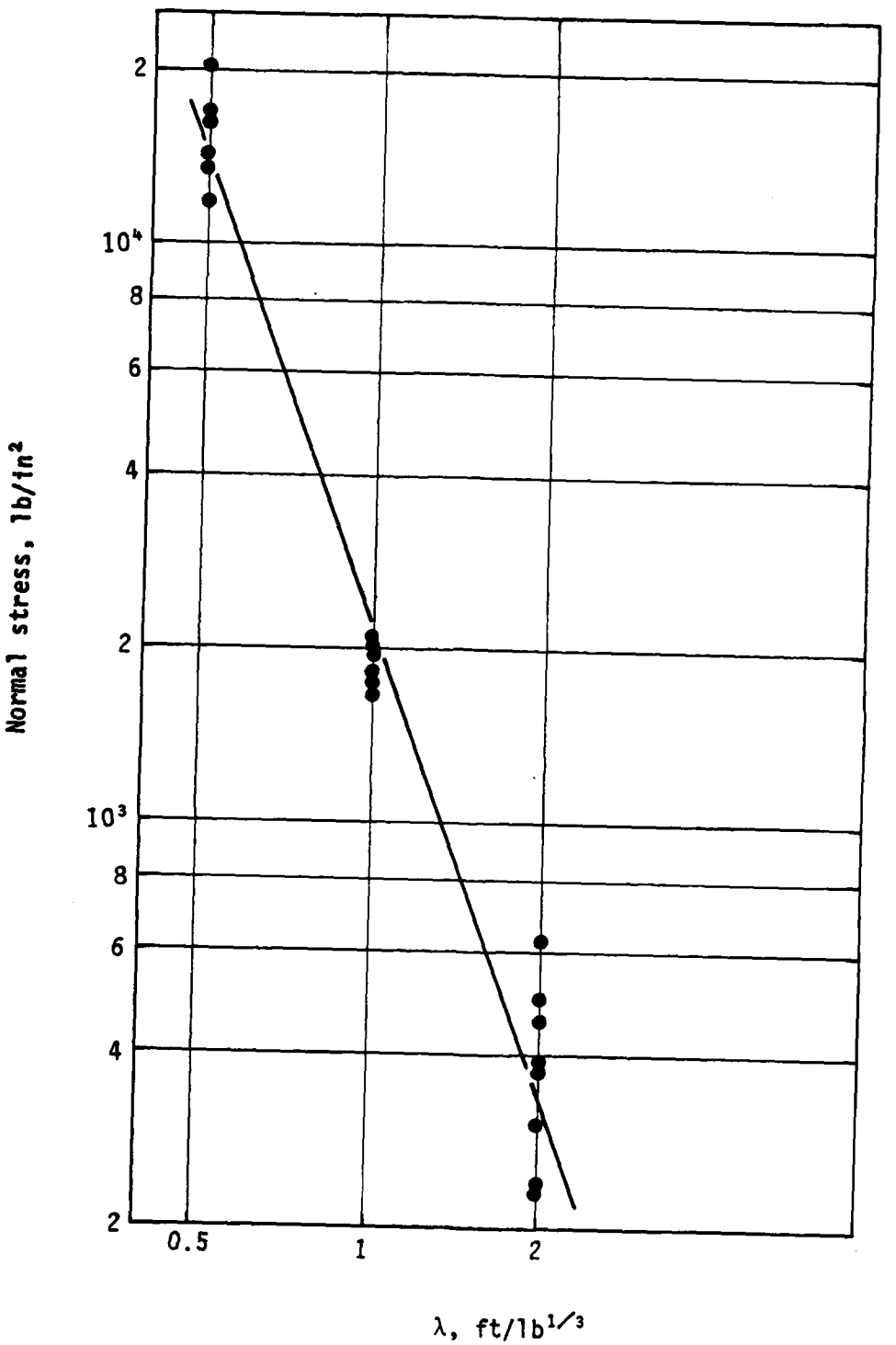

Figure 24. Data for Tests Without a Burster Slab.

The best-fit equation for these data is

$$\sigma = 2{,}100\ \lambda^{-2.684} \qquad (5)$$

for which the correlation coefficient is 0.99. The standard error of estimate for the attenuation factor is 0.096 and 0.0234 for the logarithm of the intercept.

A discussion of the results presented in this section is included in Section V.

(The reverse of this page is blank.)

SECTION V
DISCUSSION OF RESULTS

FREE-FIELD, NORMAL STRESS

A plot of the best-fit line for the normal stress scaled distance (σ versus λ) relationship, for the tests without a burster slab, is shown as Figure 25a. The line labeled Data is Equation (5) presented in the former section. _____ this line is the predicted preshot relationship which was used to set instrumentation levels. The predicted relationship is an average of predictions derived from (1) the nonnuclear design manual ($\rho_2 C_2$ = 5,168 lb-s/ft^3, coupling factor = 0.7 TNT), (2) a compilation of high-explosive test events, and (3) data in Reference 1. Figure 25a shows good agreement between the predictions and the actual measurements.* Figure 25a is a replot of Figure 24. A review of Figure 24 reveals that the best-fit line [Equation (5)] passes slightly above the data points at $\lambda = 1$. This suggests that a curvilinear relationship might better fit the data. It might also suggest that a break (change in slope) occurs in the linear relationship so that the function remains linear, but becomes steeper at $\lambda < 0.5$. Such a trend is well known. However, concern must be expressed over the range in the data at $\lambda = 2$. At the low stress levels associated with $\lambda = 2$ the pressure sensors were exposed to a stress on the order of 0.05 percent of their range (50-kilobars), and nearly 0.5 kilobar below the nearest calibration pressure. However, real concern is not expressed over this point, because the tests without a burster slab were performed only to confirm the attenuation determined for the tests having a burster slab in the test configuration.

Figure 25b is a plot which presents a comparison between the results for the tests without a burster slab ($\sigma = 2100\ \lambda^{-2.684}$) and the results for the tests with a burster slab ($\sigma = 5879\ \lambda^{-1.325}$). The two lines shown are graphical representations of these best-fit equations. As noted, the effect of the

*Items (1) and (2) were provided by Applied Research Associates, Incorporated of Albuquerque, New Mexico. This firm provided general consultation to the principal investigator on this study. The prediction equation is only valid for lambda between 2 and 15. However, because no known data existed in the range of $0.5 < \lambda < 2$, the prediction equation was arbitrarily extended into this range to provide an estimate of anticipated normal stress for stress gage calibration, center frequencies, and band-edge calibrations.

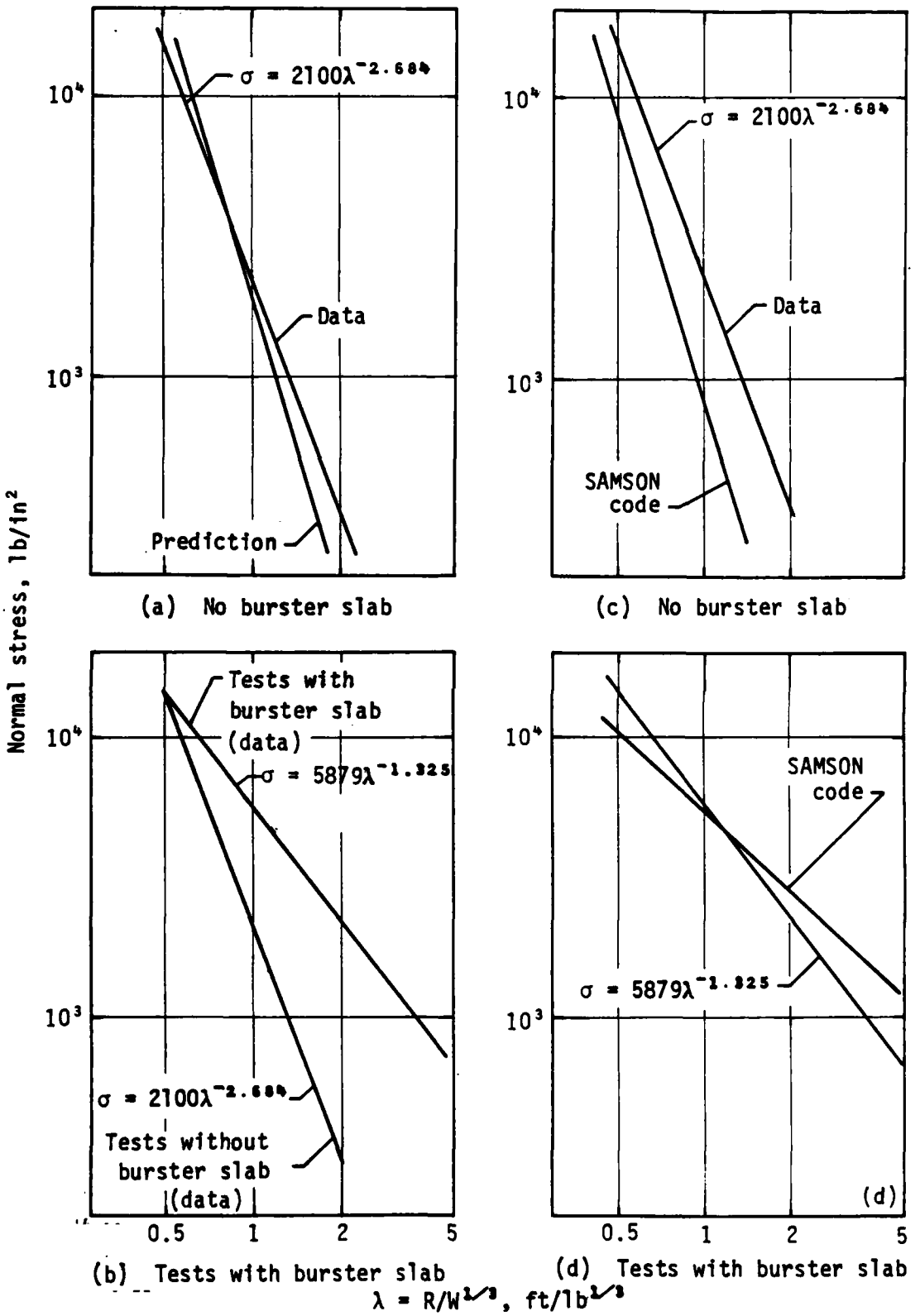

Figure 25. Comparison of Test Results, Predictions, and SAMSON Code Values.

burster slab is that of increased stress at $\lambda > 0.5$. Apparently, the higher seismic wave speed in the burster slab creates more of a planar shock front in the sand as suggested by a -1.325 attenuation factor.

A series of two-dimensional calculations was performed to support the conclusion drawn from the tests with a burster slab present; namely, the attenuation rate is best described by planar divergence. The two-dimensional calculations were performed using the finite element code SAMSON (Reference 8). SAMSON is based on a small-strain formulation and was developed primarily for soil structure interaction analysis. The finite element mesh for this problem was axisymmetric about the centerline of the cylindrical explosive. Triangular and quadrilateral elements were used in the mesh. The boundaries of the mesh were located at a distance sufficiently removed from the target points to avoid reflections returning to the region of interest.

Due to the high pressures involved in the explosive elements, severe mesh distortions occurred. In an effort to reduce these distortions the elements immediate to the explosive elements were treated as linearly elastic with a somewhat arbitrary increased stiffness. This adjustment may be rationalized on the basis that the mathematical models for the sand and concrete do not correctly represent the behavior at high strain rates. The explosive was modeled using the Jones-Wilkins-Lee Equation of State (Reference 9); the AFWL engineering model was used for the sand.

The SAMSON code results are shown along with the experimental results in Figures 25c and 25d. Figure 25c reveals that the blast pressure attenuation can be reasonably computed by means of the code. This figure further demonstrates that the predicted values of normal stress, the experimental values, and those computed via SAMSON are in reasonably good agreement. The calculations indicated in Figure 25d support the data and reinforce the conclusion--that of near planar divergence for the tests with a burster slab.

As mentioned in Section IV, the data in the σ,λ-plane do not contain any gravity effects. That is, the $W^{1/3}$ term in the denominator of λ is actually $(W_m \cdot G^3)^{1/3}$ and the numerator is $R_m \cdot G$; thus the gravity terms theoretically cancel. A numerical analysis of the σ versus λ data could not detect any statistic revealing any gravitational effects. However, if normal stress

is plotted versus range (dimensional), then the influence of gravity, as it affects explosive yield, is clearly shown. Figure 26 is such a plot for the burster-slab data. This figure was constructed from the least-squares equation for the burster-slab data and it is based on the assumption that the phenomenon under study is described by the surface shown in Figure 6, Section III. As noted in Section IV, this assumption is valid, except at $\lambda = 0.5$ due to an oversight in the experimental design. The normal stress in Figure 26 is defined by

$$\sigma = 9326\ (R)^{-1.325} \cdot [G(W)^{1/3}]^{1.241} \tag{6}$$

where

σ = normal stress, lb/ft^2

R = range, feet

$G(W)^{1/3}$ = gravity-scaled yield, $ft\text{-}s^{-2} \cdot lb^{1/3}$

Figure 27 is a plot of scaled duration and impulse from selected stress histories. Only a few of the data traces were suitable for determination of the characteristics (duration, t_D, and impulse, I) of the first positive cycle. Many of the records contained reflected impulses and most exhibited a zero offset.

The slope of the scaled duration relationship is in essential agreement with near-field data presented by Higgins et al. (Reference 3) for a planar explosive array. The increase in t_D in the near-field ($\lambda < 6$) is apparently due to the rapid attenuation of the high-frequency components of the stress wave. In the far field ($\lambda > 10$) the stress wave should propagate at a near constant frequency; thus, for a planar configuration, the functional relationship between scaled time ($t_D \cdot W^{-1/3}$) and scaled distance (λ) would most likely be a growth curve having as an upper bound a value of $t_D \cdot W^{-1/3}$ on the order of 0.1.

The following equations were derived from Figure 27:

$$t_D \cdot W^{-1/3} = 0.0075\ \lambda^{0.845} \tag{7}$$

$$I \cdot W^{-1/3} = 11.7\ \lambda^{-0.332} \tag{8}$$

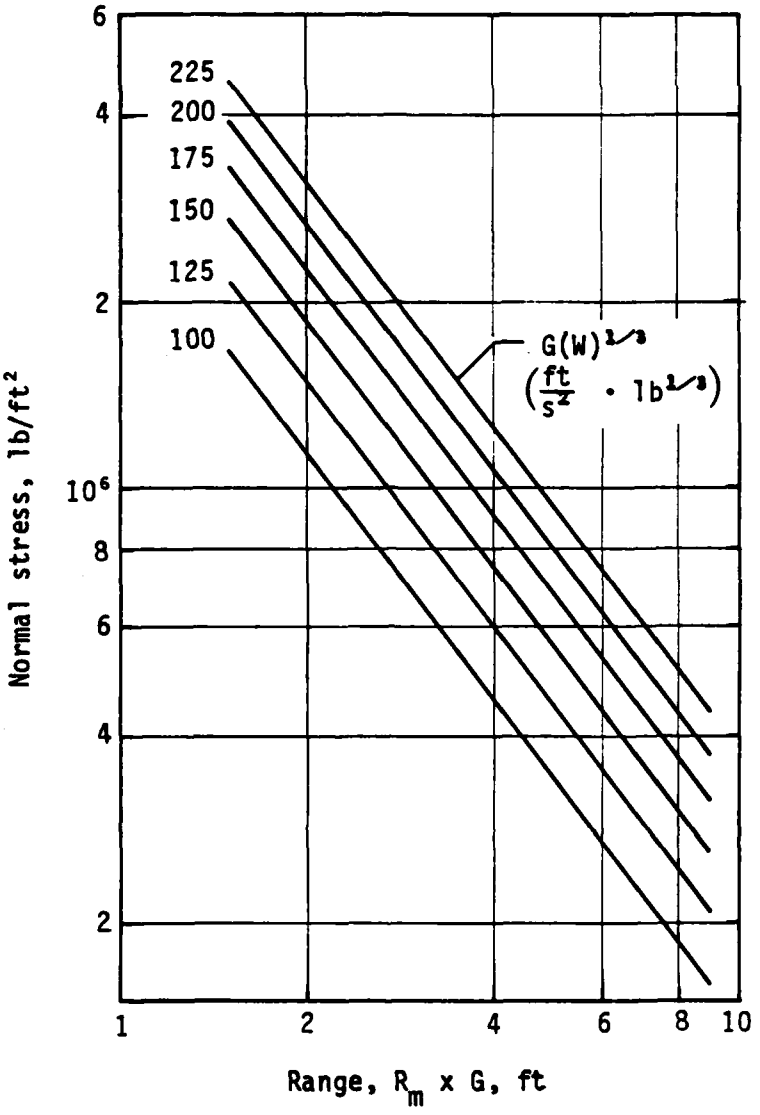

Figure 26. Influence of Scaled Energy on Normal Stress and Range With Burster Slab.

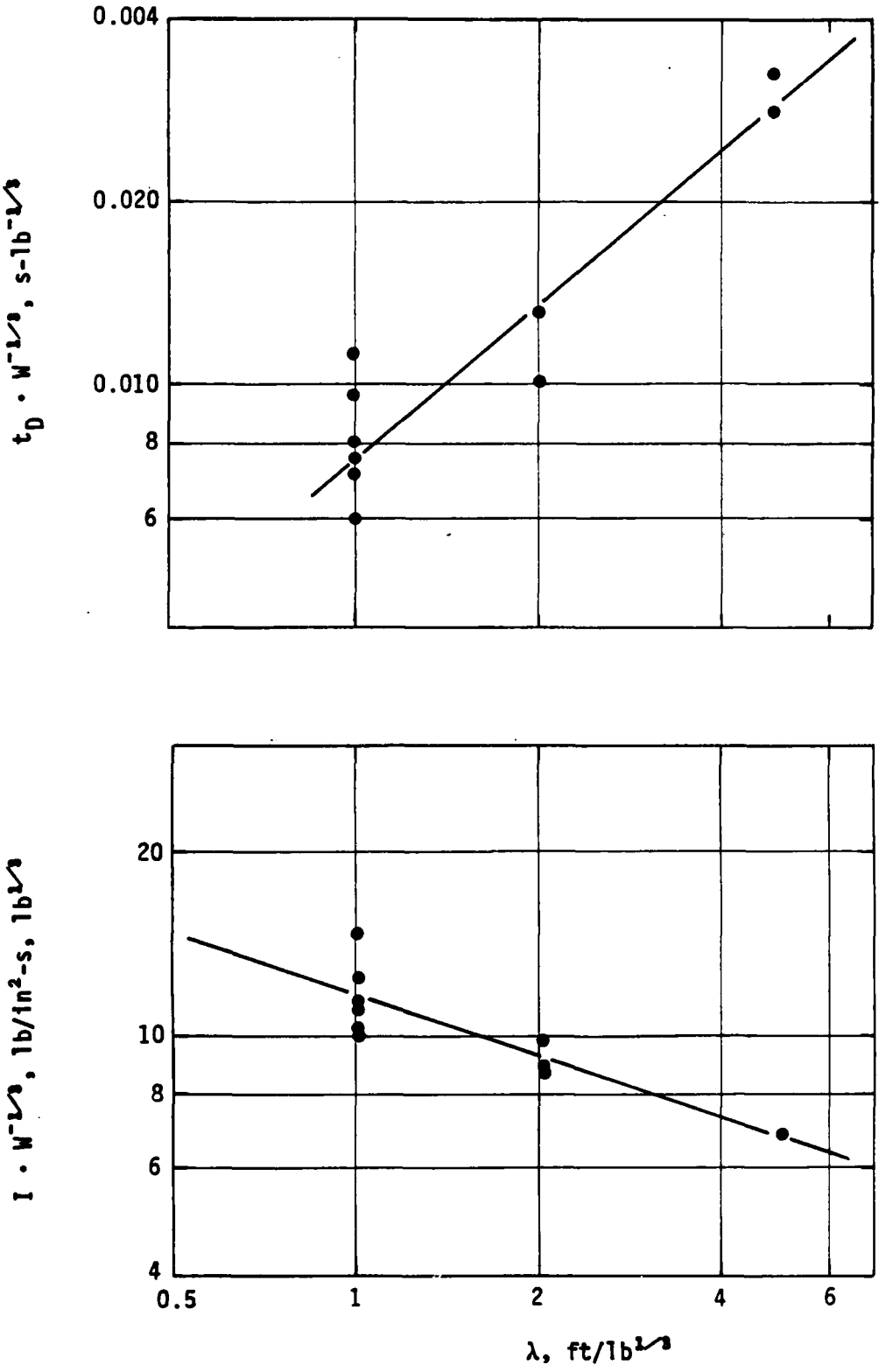

Figure 27. Scaled Duration and Impulse of Outward-Phase Duration.

where

$t_D \cdot W^{-1/3}$ = scaled duration of the first positive cycle, $s\text{-}lb^{-1/3}$

$I \cdot W^{-1/3}$ = scaled impulse of the first positive cycle $lb/in^2\text{-}s \cdot lb^{-1/3}$

λ = scaled distance, $ft\text{-}lb^{-1/3}$

CONCLUSIONS

The purpose of this study was to evaluate the suitability of a centrifuge as a device on which blast parameters could be evaluated on a small scale. The particular problem studied was concerned with the simulation of blast parameters in a sand continuum beneath a reinforced concrete burster slab. Due to the state of the art in miniature instrumentation development, the only blast parameter that could be evaluated was normal stress. Normal stress was measured using a carbon-foil pressure sensor mounted on stainless steel shim stock. In reality the development of a normal stress gage was part of this study. The particular gage configuration selected was based primarily upon size considerations to be consistent with the concept of a point measurement in a high G-level acceleration field. Following a trial development period, during which the final gage configuration evolved, the gage performed successfully.

The convincing proof of the suitability of the centrifuge as a blast-parameter simulator is revealed by the results presented in Figure 25a. Here the data for the tests without a burster slab present are in essential agreement with the preshot predictions. The predictions were derived from an extensive data base collected over several decades of ground motion research.

The results presented for the tests, which included a burster slab, reveal a signficantly different attenuation rate than that determined for the tests without a burster slab. The replication in the data does not support the conclusion that this difference is due to experimental error or gravitational effects. Rather, the differences are due to the burster slab, which alters the shape of the wavelength from spherical to planar divergence. The phenomenological differences observed are further supported by the calculational effort, which indicated significantly different attenuation rates for the two test configurations.

The use of a centrifuge as a simulator for the determination of blast parameters appears to be a workable concept. The simulation of large high-explosive effects through gravity scaling permits the use of small charges in an experimetal device that is easily refurbished after each test. A larger centrifuge would permit the use of larger test objects and reduce the effects of reflected waves on the pressure-time histories. Also, a newer centrifuge could be properly instrumented to handle low-voltage data channels and to isolate them from deleterious high-frequency effects. These problems notwithstanding, this study does demonstrate that a centrifuge can be used to evaluate free-field blast parameters (normal stress).

REFERENCES

1. **Effects of Impact and Explosion,** National Defense Research Council, Division 2, Volume I, Washington, DC, 1946.

2. Bridgeman, P. W., **Dimensional Analysis,** Yale University Press, New Haven, CT, Revised Edition, 1937.

3. Higgins, C. J., Johnson, R. L., and Triandafilidas, G. E., **The Simulation of Earthquake-Like Ground Motions With High Explosives,** Final Report No. CE-45(78)NSF-507-1, National Science Foundation, Work performed at University of New Mexico, Department of Civil Engineering and Bureau of Engineering Research, July 1978.

4. **Engineering Study - Basket Pivot Points,** Genisco Technology Corporation, #101-95, Compton, CA, November 25, 1981.

5. **Handbook of Operation, Service, and Maintenance Instructions for Model E18J Serial No. 11,** Genisco, Inc., Los Angeles, CA, 1958.

6. **Explosives Facility License,** Civil Engineering Research Facility, AFWL (AFSC), License No. 81-22, AFWL/SE, Albuquerque, NM, November 20, 1981.

7. Moussa, A., **Die Zusammendruckbarkeit von Sand,** Mitteilungen aus dem Institut fur Verkehrswasserbau, Grundbau und Bodenmechanik, der Technischen Hochschule, Aachen, Germany, 1961.

8. Bartel, H. D., and Cole, D. M., **User Manual for SAMSON and FAMILY,** AFWL Technical Note No. DE-TN-74-009, Air Force Weapons Laboratory, Kirtland Air Force Base, NM, December 1974.

9. Dobratz, Brigitta M., **Properties of Chemical Explosives and Explosive Simulants,** Chapter 8, UCRL-51319 Rev. 1, Lawrence Livermore Laboratory, University of California/Livermore, July 1974.

(The reverse of this page is blank.)

BIBLIOGRAPHY

Abbott, P. A., **Calibration of a Vertical Shock Tube and Its Associated Soil Bin**, AFWL-TR-66-134. Air Force Weapons Laboratory, Kirtland Air Force Base, NM, August 1967.

Abrahamson, G. R., Lindberg, H. E., and Bruce, J. R., **Simulation of Strong Earthquake Motion with Explosive Line Source Arrays**, ENV76-23273, Final Report, National Science Foundation, Washington, DC, October 1977.

Adams, P. H., Ault, R. L., and Fulton, D. L., **The Sandia National Laboratories 8.8-Metre (29-Foot) and 10.7-Metre (35-Foot) Centrifuge Facilities**, SAND80-0481, Sandia Laboratories, Centrifuge, Climatic, Radiant Heat Division 1531, Albuquerque, NM, May 1980.

Albritton, G. E., **Description, Proof Test, and Evaluation of Blast Load Generator Facility**, Technical Report No. 1-707, U. S. Army Engineer Waterways Experiment Station, Corps of Engineers, Vicksburg, MS, December 1975.

Albritton, G. E., **Behavior of Flexible Cylinders Buried in Sand under Static and Dynamic Loading**, Technical Report No. 1-821, U. S. Army Engineer Waterways Experiment Station, Corps of Engineers, Vicksburg, MS, April 1968.

Al-Hussaini, Mosaid M., Goodings, Deborah J., Schofield, Andrew N., and Townsend, Frank C., "Centrifuge Modeling of Coal Waste Embankments," **Journal of the Geotechnical Division**, GT4, April 1981, pp. 481-499.

Allen, R. T., Bjork, R. L., and Gaffney, E. S., **Centrifuge Simulation of Large Yield Cratering Events**, DNA 4611F, Defense Nuclear Agency, Washington, DC, 30 December 1977.

Analysis of Free-Field Data in a Half-Space under Dynamic Loads, Project No. 1080, Task No. 108001, prepared by MRD Division, General American Transportation Corporation for Air Force Special Weapons Center, Kirtland Air Force Base, NM, February 15, 1964.

Anderson, D., **The Feasibility of Generating Various Desired Pressure Wave Forms in Shock Tubes Through the Successive Detonation of Explosive Charges**, AFSWC-TN-57-27, Air Force Special Weapons Center, Kirtland Air Force Base, NM, August 1958.

Banister, John R., Pyke, Robert, Ellett, Maxwell, and Winters, Leon, "In-Situ Pressure Measurements at Rio Blanco," **Journal of the Geotechnical Engineering Division**, Proc., Paper 12471, Vol. 102, No. GT10, October 1976.

Baron, M. L., Skalak, R., and Lecht, C. P., "Particle-in-Cell Method Studies and Their Applications," **Journal of the Engineering Mechanics Division, American Society of Civil Engineers**, Vol. 91, No. EM3, June 1965, pp. 129-145.

Bassett, R. J., and Horner, J., "¢1. Prototype deformations from centrifugal model tests," **Sampling Techniques and Laboratory Measurement**.

Baum, Carl E., BAS Sensor Notes, Note 2, Inductive Techniques Using Uniform Transmission-Line Structures for Measuring Eulerian Position in Lagrangian-Flow Shock Waves in High-density Media, Air Force Weapons Laboratory, Kirtland Air Force Base, NM, September 9, 1978.

Baum, Dennis (Project Manger), **Feasibility of Magnetic Velocity Gage for DABS Tests**, Final Report 122, Civil Engineering Research Facility, November 1976. (By Artec Associates Inc., 26046 Eden Landing Road, Hayward, CA.)

Baum, Neal, **Carbon-Manganin Gage Development**, AFWL-TR-80-54, Air Force Weapons Laboratory, Kirtland Air Force Base, NM, November 1980.

Baum, Neal P., BAS Sensor Notes, Note 1: Instrumentation Evaluation for Surface Bursts in Underground Cavities, Civil Engineering Research Facility, University of New Mexico, June 1973.

Baum, Neal and Edgel, W. Reed, **Instrumentation Development for the Trench Series**, AFWL-tR-79-171, Air Force Weapons Laboratory, Kirtland Air Force Base, NM, 1980.

Bratton, James L., **Effects of Material Properties on Cylindrical Wave Propagation in Geologic Materials**, AFWL-TR-77-184, prepared for Defense Nuclear Agency, Washington, DC, and Air Force Weapons Laboratory, Kirtland Air Force Base, NM, October 1978.

Bruce, J. R., and Lindberg, H. E., "Earthquake Simulation Using Contained Explosions," Paper presented at Specialty Conference, American Society of Civil Engineers, Atlanta, GA, January 1981.

Bruce, J. R., Lindberg, H. E., and Abrahamson, G. R., **Simulation of Strong Earthquake Motion wiht Contained-Explosive Line Source Arrays**, PFR 78-0093, Interim Report, National Science Foundation, Washington, DC, March 1979.

Brucham, Richard L., **Evaluation of Piezoelectric Polymer Soil-Stress Gage**, DE-TN-74-016, Air Force Weapons Laboratory, Kirtland Air Force Base, NM, October 1974.

Cagliostro, D. J., Florence, A. L., Abrahamson, G. R., and Nagumo, G., "Characterization of an Energy Source for Modeling Hypothetical Core Disruptive Accidents in Nuclear Reactors," **Nuclear Engineering and Design**, 27(1974), North-Holland Publishing Comapny, pp. 94-105.

Cassino, V., and Chavez, D. J., **Effect of Pavement Design on Cratering Damage from Penetrating Weapons**, AFWL-TR-74-197, Air Force Weapons Laboratory, Kirtland Air Force Base, NM, October 1975.

Chabai, Albert J., "On Scaling Dimensions of Craters Produced by Buried Explosives," **Journal of Geophysical Reserch**, Vol. 70, No. 20, October 15, 1965, pp. 5075-5098.

Chae, Y. S., **Dynamic Pressure Distribution at the Base of a Rigid Footing Subjected to Vibratory Loads**, Report No. 3-88, U. S. Army Engineer Waterways Experiment Station, Corps of Engineers, Vicksburg, MS, May 1964.

Chambers, B. S., and Hasdal, J. A., **Estimates of Thermal Radiation Environments for Planning a Thermal Simulation on a HE Test,** DNA 5073F, Defense Nuclear Agency, Washington, DC, March 1979.

Change, N. D., **General Guide to ICP Instrumentation,** G-0001, PCB Piezotronics, Inc., P.O. Box 33, Buffalo, N.Y.

Chou, Pei Chi and Hopkins, Alan K. (editors), **Dynamic Response of Materials to Intense Impulsive Loading,** AD-768 416, Air Force Materials Laboratory, Wright-Patterson Air Force Base, Ohio, August 1972.

Christian, J. T., **Two-Dimensional Analysis of Stress and Strain in Soils, Report 1: Iteration Procedure for Saturated Elastic Porous Material,** Contract Report No. 3-129, U.S. Army Engineer Waterways Experiment Station, Corps of Engineers, Vickburg, MS, June 1965.

Clark, G. B., Rupert, G. B., and Jamison, J. E., **A Comparison of Plane and Spherical Transient Volt Waves with Explosive Generated Waves in Rock Masses,** Report No. 1-170, U.S. Army Engineer Waterways Experiment Station, Corps of Engineers, Vickburg, MS, April 1967

Coleman, P. L. and Kratz, H. R., XBHUSSAR SWORD Series, HYBLA GOLD Event; Plasma, Ablation and Pipe Expansion Measurements, POR 7010 (WT-7010), Defense Nuclear Agency, Washington, DC, February 1, 1979.

Crawford, Robert E., Romesberg, Laverne E., Wilson, Leroy E., and Schreyer, Howard L., **Protection from Nonnuclear Weapons,** AFWL-TR-70-127, Air Force Weapons Laboratory, Kirtland Air Force Base, NM, February 1971.

Davis, R. O. and Mullenger, G., **Rate-Type Fluid Model for Granular Media with a Critical State,** CERF DP/EM-6, Air Force Weapons Laboratory, Kirtland Air Force Base, NM, February 1977.

Dawson, Maynard H. and Rechlin, Floyd F., **100 GHz Diagnostic Imaging Techniques,** DARE Technology, Inc., San Diego, CA.

De Carli, P. S., **Stress-Gage System for the Megabar (100 GPa) Range,** DNA 4066 F, Defense Nuclear Agency, Washington, DC, June 1976.

Divoky, David, "The Equivalent of Mass and Energy Scaling of Crater Dimensions: Comment on a Paper by A. J. Chabai," **Journal of Geophysical Research,** Vol. 71, No. 10, May 15, 1966, p. 2691.

Dorris, A. F., And Albritton, G. E., **Response of a Buried Prototype Communications Conduit to Static and Dynamic Loading,** Technical Report No. 1-750, U.S. Army Engineer Waterways Experiment Station, Corps of Engineers, Vickburg, MS, December 1966.

Drnevich, V. P., Hall J. R., Jr., and Richart F. E., Jr., **Transient Loading Tests on a Rigid Circular Footing,** Contract Report No. 3-146, U.S. Army Engineer Waterways Experiment Station, Corps of Engineers, Vickburg, MS, February 1966.

Drnevich, V. P., Hall, J. R., Jr., and Richart, F. E., Jr., **Large Amplitude Vibration Effects on the Shear Modulus of Sand**, Report No. 3-161, U.S. Army Engineer Waterways Experiment Station, Corps of Engineers, Vickburg, MS, October 1966.

Durbin, W. L., **Study of the Dynamic Stress-Strain and Wave-Propagation Characteristics of Soils, Report 3: Measurements of Stress-Strain, Peak Particle Velocity, and Wave-Propagation Velocity in Three Sands**, Contract Report No. 3-91, U.S. Army Engineer Waterways Experiment Station, Corps of Engineers, Vickburg, MS, February 1965.

Durbin, W. L., **Study of the Dynamic Stress-Strain and Wave-Propagation Characteristics of Soils, Report 2: Correlation of Stress-Strain and Wave-Propagation Parameters in Shock-Loaded Dry Sands**, Contract Report No. 3-91, U.S. Army Engineer Waterways Experiment Station, Corps of Engineers, Vickburg, MS, November 1964.

Environmental Capability, prepared by Environmental Branch (FTSE), for Technical Services Division, 4900th Test Group (Flight Test), Air Force Special Weapons Center, Air Force Systems Command, Kirtland Air Force Base, NM, Updated October 1972.

Ericsson, V., and Edin, K., "On Complete Blast Scaling," **The Physics of Fluids**, Vol. 3, No. 5, September-October 1960, pp. 893-895.

Evaluation Testing of Rotational Velocity Transducers-Sparton S.W. Inc. Model 605, Concepts Inc. Model 2001-22, Technical Note No. AFWL/DE-TN-73-023, Air Force Weapons Laboratory, Kirtland Air Force Base, NM, May 1973.

Farhoomand, I. and Wilson, E., **A Nonlinear Finite Element Code for Analyzing the Blast Response of Underground Structures**, Contract Report N-70-1, U.S. Army Engineer Waterways Experiment Station, Vicksburg, MS, January 1970.

Faust, R. W. and Ingram, J. K., **Development of On-Structure Stress Gages**, Technical Report No. 1-801, conducted by U.S. Army Engineer Waterways Experiment Station, Corps of Engineers, Vicksburg, MS, sponsored by Defense Atomic Support Agency, November 1967.

Fernandez, Herbert M. (Symposium Manager), **Instrumentation for Nuclear Weapon Effects Simulation Symposium, Volume I: Electromagnetic Pulse**, AFSWC-TR-70-5, Vol. I, Air Force Special Weapons Center, Kirtland Air Force Base, NM, March 1970.

Fernandez, Herbert M. (Symposium Manager), **Instrumentation for Nuclear Weapon Effects Simulation Symposium, Volume II: Shock Effects**, AFSWC-TR-70-5, Vol. II, Air Force Special Weapons Center, Kirtland Air Force Base, NM, March 1970.

Fernandez, Herbert M. (Symposium Manager), **Instrumentation for Nuclear Weapon Effects Simulation Symposium, Volume III: Transient Radiation Effects on Electronic Systems**, AFSWC-TR-70-5, Vol. III, Air Force Special Weapons Center, Kirtland Air Force Base, NM, March 1970.

Fernandez, Herbert M. (Symposium Manager), **Instrumentation for Nuclear Weapon Effects Simulation Symposium, Volume IV: General Instrumentation,** AFSWC-TR-70-5, Vol. IV, Air Force Special Weapons Center, Kirtland Air Force Base, NM, March 1970.

Ferritto, John M., **Dynamic Tests of Model Concrete,** Technical Report R-650, Sponsored by Defense Atomic Support Agency, Clearinghouse for Federal Scientific & Technical Information (CFSTI), 5285 Port Royal Road, Springfield, VA 22151, November 1969.

Fogelson, David J., **Ground Motion Transducer Placement System,** AFWL-TR-76-310, Air Force Weapons Laboratory, Kirtland Air Force Base, NM, February 1977.

Four Papers Concerning Recent Work on Ground Motion Measurements, SC-R-65-904, Sandia Corporation, Technical Information Division III, Albuquerque, NM, April 1965.

A. Perret, W. R., "Ground Motion Measurements."

B. Wistor, J. W., "An Extended Range Velocity Gage for Measurements in High Shock Environments."

C. Hansen, G. J., "Electronic Integrators for Intrumentation Applications."

D. Palmer, D. G., "Instrumenting Nuclear Explosions."

Fugelso, L. E. (Project Engineer), **Analytical Study of Early Deformation from an Underground Explosion,** DASA Report No. 1297, prepared by Mechanics Research Division, American Machine & Foundry Company, Niles, Illinois, for the Defense Atomic Support Agency, 1962.

Goldsmith, W., Polivka, M., and Yang, T., "Dynamic Behavior of Concrete," **Experimental Mechanics,** Vol. 6, No. 2, February 1966, pp. 65-79.

Hadala, P. F., **Dynamic Bearing Capacity of Soils: Report No. 4--Investigation of a Dimensionless Load-Displacement Relation for Footings on Clay,** Technical Report No. 3-599, U.S. Army Engineer Waterways Experiment Station, Corps of Engineers, Vickburg, MS, June 1965.

Haltiwanger, J. D., Hall, W. J., and Newmark, N. M., **Approximate Methods for the Vulnerability Analysis of Structures Subjected to the Effects of Nuclear Blast, Volume I (Chapters 1 through 4),** Report No. U-275-76, N.M. Newmark Consulting Engineering Services, Urbana, Illinois, June 15, 1976.

Hampton, Delon, **A Study of Pore Air Pressures Generated in Soil Subjected To Air Shock Waves,** WL-TDR-64-3, Air Force Weapons Laboratory, Research and Technology Division, Kirtland Air Force Base, NM, October 1964.

Hampton, Delon and Truesdale, William B., "Stress and Strain Gages for Use in Soil Dynamic Research," Preprint No. P19-3-PHYMMID-67, **22nd Annual ISA Conference and Exhibit,** Chicago, Illinois, September 11-14, 1967.

Hardin, B. O. and Richart, F. E., Jr., "Elastic Wave Velocities in Granular Soils," **Journal of the Soil Mechanics and Foundations Division,** American Society of Civil Engineers, Vol. 89, No. SM1, Proc. Paper 3407, February 1963, pp. 33-65.

Harkin, J. B. (Project Engineer, MRD Division, General American Transportation Corp.), **Theoretical Study of Energy Distribution in a Half-Space under Dynamic Loads,** AFSWC-TDR-62-43, Air Force Special Weapons Center, Kirtland Air Force Base, NM, July 1962.

Hendron, A. J., Jr., **Correlation of Operation Snowball Ground Motions with Dynamic Properties of Test Site Soils,** conducted by U.S. Army Engineer Waterways Experiment Station, Corps of Engineers, Vicksburg, MS, sponsored by Office, Chief of Engineers, U.S. Army and Defense Atomic Support Agency, October 1965.

Hobbs, Norman P., and Wetmore, Kenneth R., **PIVUL--A Computer Code for Rapid Assessment of the Vulnerability of Simple Structures to Blast,** Contract Report ARBRL-CR-00417, U.S. Army Armament Research & Development Command, U.S. Army Ballistic Research Laboratory, ATTN:DRDAR-BL, Aberdeen Proving Ground, MD, March 1980.

Hoff, G. C., **Investigation of Expanding Grout and Concrete, Report 1, Summary of Field Mixture Test Results, July 1969 through June 1970,** Miscellaneous Paper C-71-5, conducted by U.S. Army Engineer Waterways Experiment Station, Vicksburg, MS, sponsored by U.S. Atomic Energy Commission-Sandia Laboratories, and Test Command, Defense Atomic Support Agency, June 1971.

Hoff, George C., **Cellular Concrete Studies; Report 2, Evaluation of Crushed Cellular Concrete,** Miscellaneous Paper C-74-8, Report 2, U.S. Atomic Energy Commission, Sandia Laboratories, P.O. Box 5800, Kirtland Air Force Base, NM, December 1974.

Hokanson, Lawrence Dale, **Soil Property Effects on Bomb Cratering in Pavement Systems,** AFWL-TR-72-231, Air Force Weapons Laboratory, Kirtland Air Force Base, NM, February 1973.

Holsapple, K. A., and Schmidt, R. M., "A material-strength model for apparent crater volume," **Proc. Lunar Planet. Sci. Conf. 10th,** 1979, pp. 2757-2777.

Huff, W. L., **Test Devices Blast Load Generator Facility,** Miscellaneous Paper N-69-1, U.S. Army Engineer Waterways Experiment Station, Corps of Engineers, Vicksburg, MS, April 1969.

Jackson, John G., Jr., **Material Response Characterization,** Miscellaneous Paper S-77-11, Defense Nuclear Agency, Washington, DC, August 1977.

Jackson, J. G., Jr., Physical Property and Dynamic Compressibility Analysis of the Watching Hill Blast Range, conducted by U. S. Army Engineer Waterways Experiment Station, Vicksburg, MS, sponsored by Defense Nuclear Agency and Office, Chief of Engineers, U. S. Army, April 1972.

Jackson, J. G., Jr., **Analysis of Labortory Test Data To Derive Soil Constitutive Properties**, paper presented at the Defense Atomic Support Agency (DAS) Strategic Structures Vulnerability/Hardening Long Range Planning Meeting, U. S. Army Engineer Waterways Experiment Station, Vicksburg, MS, January 14-16, 1969.

Jackson, J. G., Jr., Ehrgott, J. Q., and Rohani, Behzad, **Loading Rate Effects on Compressibility of Sand**, Miscellaneous Paper SL-79-24, Structures Laboratory, U. S. Army Engineer Waterways Experiment Station, Vicksburg, MS, prepared for Defense Nuclear Agency, Washington, DC, November 1979.

Janza, F. J., and Hicks, C. W., **The Calibration and Interpretation of Recorded Sock-Tube Pressure Data Using Piezoelectric Sensors**, Technical Documentary Report No. RTD-TDR-63-3073, Research and Technology Division, Air Force Weapons Laboratory, Kirtland Air Force Base, NM, November 1963.

Kennedy, J. E., "Explosive Output for Driving Metal," **12th Annual Symposium: Behavior and Utilization of Explosives in Engineering Design**, New Mexico Section American Society of Mechanical Engineers and the University of New Mexico College of Engineering, Albuquerque, NM, March 2-3, 1972, pp. 109-124.

Koester, K. L., Kosowsky, L. H., and Sparacio, J. G., **An Experimental Millimeter Monopulse Track Radar**, Norden Division, United Aircraft Corporation, Norwalk, Connecticut.

Kondner, R. L., **A Rheologic Investigation of the Dynamic Response Spectra of Cohesive Soils--Summary Report**, Report No. 3-148, U. S. Army Engineer Waterways Experiment Station, Corps of Engineers, Vicksburg, MS, November 1965.

Lawrence, R. J. and Mason, D. S., **WONDY IV--A Computer Program for One-Dimensional Wave Propagation with Rezonining**, SC-RR-710284, Code Application Division, 5166, Sandia Laboratories, Albuquerque, NM, August 1971.

Matthews, A. T., Sandler, I., and Bleick, H. H., **Investigation of Ground Shock Effects in Nonlinear Hysteretic Media, Report 4: Effect of a Step Load Moving with Constant Superseismic Velocity on a Half-Space of a Variable Modulus Material**, Contract Report S-68-1, U. S. Army Engineer Waterways Experiment Station, Corps of Engineers, Vicksburg, MS, March 1970.

McNeill, Robert L., **A Study of the Propagation of Stress Waves in Sand**, AFWL-TR-65-180, Air Force Weapons Laboratory, Kirtland Air Force Base, NM, March 1966.

Mitchell, J. K., Shen, Chih-Kang, and Monismith, C. L., **Behavior of Stabilized Soils under Repeated Loading, Report 1: Background, Equipment, Preliminary Investigations, Repeated Compression and Flexure Tests on Cement-Treated Silty Clay**, Contract Report No. 3-145, U. S. Army Engineer Waterways Experiment Station, Corps of Engineers, Vicksburg, MS, December 1965.

Nelson, I., **Investigaton of Ground Shock Effects in Nonlinear Hysteretic Media, Report 2: Modeling the Behavior of a Real Soil**, Contract Report S-68-1, U. S. Army Engineer Waterways Experiment Station, Corps of Engineers, Vicksburg, MS, July 1970.

Nelson, I., Baron, M. L., and Sandler, I., "13. Mathematical Models for Geological Materials for Wave-Propagation Studies," **Shock Waves and the Mechanical Properties of Solids**, Syracuse University Press, Syracuse, NY., 1971.

"Nondestructive Testing of Concrete," **Highway Reserch Record**, Highway Research Board, Number 378, Washington, DC, 1972.

Palacios, N. and Kennedy, T. E., **The Dynamic Response of Buried Concrete Arches, Project 3.2 Operation Snowball**, Technical Report No. 10797, U. S. Army Engineer Waterways Experiment Station, Corps of Engineers, Vicksburg, MS, September 1967.

Pasclar, Herbert G., **Millimeter Wave Passive Sensing from Satellites**, Aerojet ElectroSystems Company, 1100 W. Hollyvale Street, Azusa, CA.

Pickett, Stephen F., and Smiel, Adalbert J., **Performance Evaluation of Velocity Measurement Systems**, Draft Report to Air Force Weapons Laboratory, Kirtland Air Force Base, NM, July 1974.

Piekutowski, A. J., **Laboratory-Scale High-Explosive Cratering and Ejecta Phenomenology Studies**, AFWL-TR-72-155, Final Report, Air Force Weapons Laboratory,Kirtland Air Force Base, NM, April 1974.

Polanin, B. P., and Washington, L. H., **Design and Instrumentation of an Earth Shock Tube**, BRL Progress Report No. 21, The Ballistic Reserch Laboratories, Aberdeen Proving Ground, Aberdeen, MD, June 1963.

Poplin, J. K., **Dynamic Bearing Capacity of Soils: Report 2--Dynamically Loaded Small-Scale Footing Tests on Dry, Dense Sand**, Technical Report No. 3-599, U. S. Army Engineer Waterways Experiment Station,Corps of Engineers, Vicksburg, MS, September 1965.

Prevost, Jean H., Cuny, Bernard, and Scott, Ronald F., "Offshore Gravity Structures: Centrifuge Modeling," **Journal of the Geotechnical Division**, GT2, February 1981, pp. 125-141.

Progress Briefing No. 1 on Subtask Statement 2.01, Blast Parameters Study, by NMERI to AFESC/RDCS, Tyndall Air Force Base, FL, April 1, 1981.

Progress Briefing No. 2 on Subtask Statement 2.01, Blast Parameters Study, by NMERI to AFESC/RDCS, Tyndall Air Force Base, FL, May 20, 1981.

Read, H. E., and Maiden, C. J., **The Dynamic Behavior of Concrete**, 3SR-707, Topical Report, Space and Missile Systems Orgnization, Air Force Systems Command, Norton Air Force Base, CA, Attn: MMNSS, August 1971.

Renick, Joseph D., Fogelson, David J., and Baum, Neal, Remote In-Material Placement of Soil Stress Gages, Civil Engineering Research Facility and Air Force Weapons Laboratory, Kirtland Air Force Base, NM.

Rogers, Earl J., **Transducer for Dynamic Soil Pressure**, Symposium on Wave Propagation and Dynamic Properties of Earth Materials, Session IV, Instrumentation and Field Investigation Techniques for Determining Dynamic Properties of Earth Materials and Assessing Foundation of Free-Field Response, Albuquerque, NM, August 23 through 25, 1967.

Sakurai, A., and Pinkston, J. M., **Water Shock Waves Resulting from Explosions above an Air-Water Interface: Report 1--Results of a Theoretical Investigation**, Technical Report No. 1-771, U. S. Army Engineer Waterways Experiment Station, Corps of Engineers, Vicksburg, MS, April 1967.

Schmidt, R. M., "A centrifuge cratering experiment: Development of a gravity-scaled yield parameter," **Impact and Explosion Cratering**, Pergamon Press, New York, 1977, pp. 1261-1278.

Schmidt, R. M., Fragaszy, R. J., and Holsapple, K. A., "Centrifuge Modeling of Soil Liquefaction Due To Airblast," presented at **Seventh International Symposium on Military Applications of Blast Simulaiton, Defence Research Establishment Suffield, Ralston, Alberta, Canada, Medicine Hat, Alberta, July 13-17, 1981.**

Schmidt, R. M., and Holsapple, K. A., "Theory and Experiments on Centrifuge Cratering," Journal of Gephysicla Research, Vol. 85, No. B1, January 10, 1980, pp. 235-252.

Schmidt, R. M. and Holsapple, K. A., "Theory and Experiments on Centrifuge Cratering," **Journal of Geophysical Research**, Vol. 85, No. B1, January 10, 1980, pp. 235-251.

Schmidt, R. M. and Holsapple, K. A., **Centrifuge Crater Scaling Experiment I, Dry Granular Soils**, DNA 4568F, Defense Nucler Agency, Washington, DC, Febraury 1, 1978.

Scott, Ronald F. and Morgan, N. R., **Feasibility and Desirability of Constructing a Very Large Centrifuge for Geotechnical Studies**, PB-272 250, National Science Foundation, Washington, DC, March 31, 1977. (NTIS, Springfield, VA.)

Seaman, L., "Determination of the dissipation parametr tan δ for the constan-tan δ model," Personal Communication from Delon Hampton (IITRI) to Lt. Jimmie L. Bratton (AFWL), December 1966.

Seaman, L., Bycroft, G. N., nd Kirebel, H. W., **Stress Propagation in Soils, Final Report--Part III**, DASA 1266-3 Defense Atomic Support Agency, Washington, DC, May 1963.

Selig, E. T., **A Review of Stress and Strain Measurement in Soil,** sponsored by the National Science Foundation and Air Force Weapons Labortory, Kirtland Air Force Base, NM.

Sidey, Robert, **A Probe for In-Situ Measurement of Dynamic Pore Pressure,** AFWL-TR-81-4, Air Force Weapons Laboratory (NTED) Kirtland Air Force Base, NM, April 1981.

Sonnenburg, Paul N. and Schulz, George, **Response Properties of an Orthogonal System of Pendulum-Type Velocity Gages,** Draft Report, Air Force Weapons Laboratory, Kirtland Air Force Base, NM, February 1973.

Swift, L. M., **Development of Soil Displacement and Strain Gages,** DASA-1267, Final Report, Defense Atomic Support Agency, Washington, DC, September 1961.

Taylor, G., "The Formation of a Blast Wave by a Very Intense Explosion: I. Theoretical Discussion, II. The Atomic Explosin of 1945," **Proceedings of the Royal Society,** Vol. 201. A. (March 22, 1950), pp. 159-186.

Thomsen, J. M., and Franzen, R. R., **Simulation of Nuclear Underwater Shock Waves Using Planar Sources: An Investigation of Feasibility,** DNA 5340F, Final Report, Defense Nuclear Agency, Washington, DC, April 1980.

Thornton, H. T., Jr., **Field Soniscope Tests of Concrete; Report 3, Ten-Year Summary of Results,** Technicl Memorandum No. 6-383, Office, Chief of Engineers, U. S. Army, March 1967. (Conducted by U. S. Army Engineer Waterways Experiment Station, Corps of Engineers, Vicksburg, MS.)

Tremba, Edward and Sitar, Kenneth, **Small-Scale Parametric Study in Modeled Deep-Basing Geologies: Analysis of Field Test Results,** AFWL-TR-80-51, Air Force Weapons Laboratory, Kirtland Air Force Base, NM, April 1980.

Wang, E. H., **Improvement in the Capabilities of the Air Force 6-Foot Shock Tube by Several Orders of Magnitude,** AFSWC-TN-59-13, Technicl Note, Air Force Special Weapons Center, Kirtland Air Force Base, NM, May 1959.

Welch, R. E., **Test/Analysis Correlations for High Explosive Tests of Strategic Structures,** Final Report, DNA 2971F, Headquarters, Defense Nuclear Agency, Washington, DC, November 1972.

Weidlinger, P., and Matthews, A. T., "Shock and Reflections in a Nonlinear Medium," **Journal of the Engineering Mechanics Division,** American Society of Civil Engineers, Vol. 91, No. EM#, June 1965, pp. 147-168.

Westine, P. S., "Explosive Cratering," **Journal of Terramechanics,** Vol. 7, No. 2, pp. 9-19, Pergamon Press, Great Britain, 1970.

Whitman, R. V., **The Response of Soils to Dynamic Loadings,** Contract Report No. 3-26, U. S. Army Engineer Waterways Experiment Station, Corps of Engineers, Vicksburg, MS, May 1970.

Wilcox, Fred P., **Development and Test of a 95 CHz Terrain Imaging Radar,** Goodyear Aerospace Corporation, Litchfield Park, AZ.

Wang, F. S., **Analysis of Velocity Gage - High Explosive Simulation Technique Tests**, Memorandum No. 6726-613, Agbabian-Jacobsen Associates, May 27, 1969.

Young, D. F., and Murphy, G., "Dynamic Similitude of Underground Structures," **Journal of the Engineering Mechanics Division**, American Society of Civil Engineers, Vol. 90, No. EM3, June 1964, pp. 111-133.

Zaccor, J. V., **Procedures for Prediction of Ground Shock Phenomena Based on One-Dimensional shock Propagation Considerations, Report 1: Procedures and Applications**, Contract Report No. 3-171, U.S. Army Engineer Waterways Experiment Station, Corps of Engineers, Vicksburg, MS, April 1967.

Zaccor, J. V., Durbin, W. L., Wallace, N. R., and Mason, H. G., **Study of the Dynamic Stress-Strain and Wave-Propagation Characteristics of Soils, Report 4: Concepts of Shock Behavior in a Granular Medium**, Contract Report No. 3-91, U. S. Army Engineer Waterways Experiment Station,Corps of Engineers, Vicksburg, MS, March 1965.

(The reverse of this page is blank.)

APPENDIX A

APPROVED CENTRIFUGAL COUNTDOWN PROCEDURE FOR EXPLOSIVE TESTING

CENTRIFUGE COUNTDOWN PROCEDURE

T - 24 h	EMCS	Notify ordnance and centrifuge personnel of two impending shots on centrifuge in Building 1001 on Kirtland West, tests to be conducted on following day.
T - 24 h	EMCS	Notify explosive safety office of shots in Building 1001 on following day.
T - 24 h	Photo	Take documentary photos of test preparation.
T - 2 h	EMCS	Transport test fixtures from CERF main facility to Building 1001.
T - 1 1/2 h	EMCS	Install the first of two (2) fixtures on centrifuge. Secure all instrumentation cables on centrifuge arms with nylon filament tape in such a manner that cables will not stretch and break under strain of high (100 g) forces.
T - 1 h	ELEC	Hook up and check out all instrumentation channels.
T - 45 min	ELEC & ORD	Dry run system--electrical and explosive. Post warning signs--clear area.
T - 30 min	ORD	Install firing module on centrifuge and place detonator in correct test position.
T - 20 min	Photo	Take preshot photos of completed, ready-for-test configuration.
T - 15 min	ORD, CENT, EMCS	Clear out centrifuge area of personnel, actuate safety switch on centrifuge, and close centrifuge pit. Ensure that door safety switches are actuated.
T - 5 min	ORD, ELEC, EMCS	Verify that all systems are ready for test sequence. Clear area topside of all personnel not involved in test.
T - 2 min	CENT and ELEC	Energize pumps and start centrifuge. When centrifuge has reached correct force, fire detonator.
T + 1 min	CENT	Shut down centrifuge and turn off all pumps. Verify centrifuge has come to a complete stop.
T + 5 min	ORD	Verify centrifuge pit area is free from explosive hazards and safe for personnel to enter. Turn <u>off</u> safety switch on centrifuge.

T + 7 min	Photo, EMCS, TC	Take postshot photographs, inspect test fixture prior to disassembly and reassembly for second test of sequence.
T + 30 min	EMCS	Begin sequence from T - 1 1/2-hour step.
T + 30 min	EMCS	After final test, notify outside personnel testing is completed for this day.

The word HOLD from any test personnel will cause the countdown to be stopped. Test will resume from T - 5 min countdown.

Hold conditions: Any malfunction of either the centrifuge, electronic, or explosive systems which would render the test procedure unsafe, or result in unacceptable test conditions

Responsible Officers:
TC - J. Nielsen
EMCS - S. Scales
CENT - P. Adams
ELEC - G. Stewart
PHOTO - M. Davila
P.I. - J. Nielsen
ORD - R. Venegas

Prepared By: _____ Approved By: _____

Date: _____ Date: _____

(The reverse of this page is blank.)

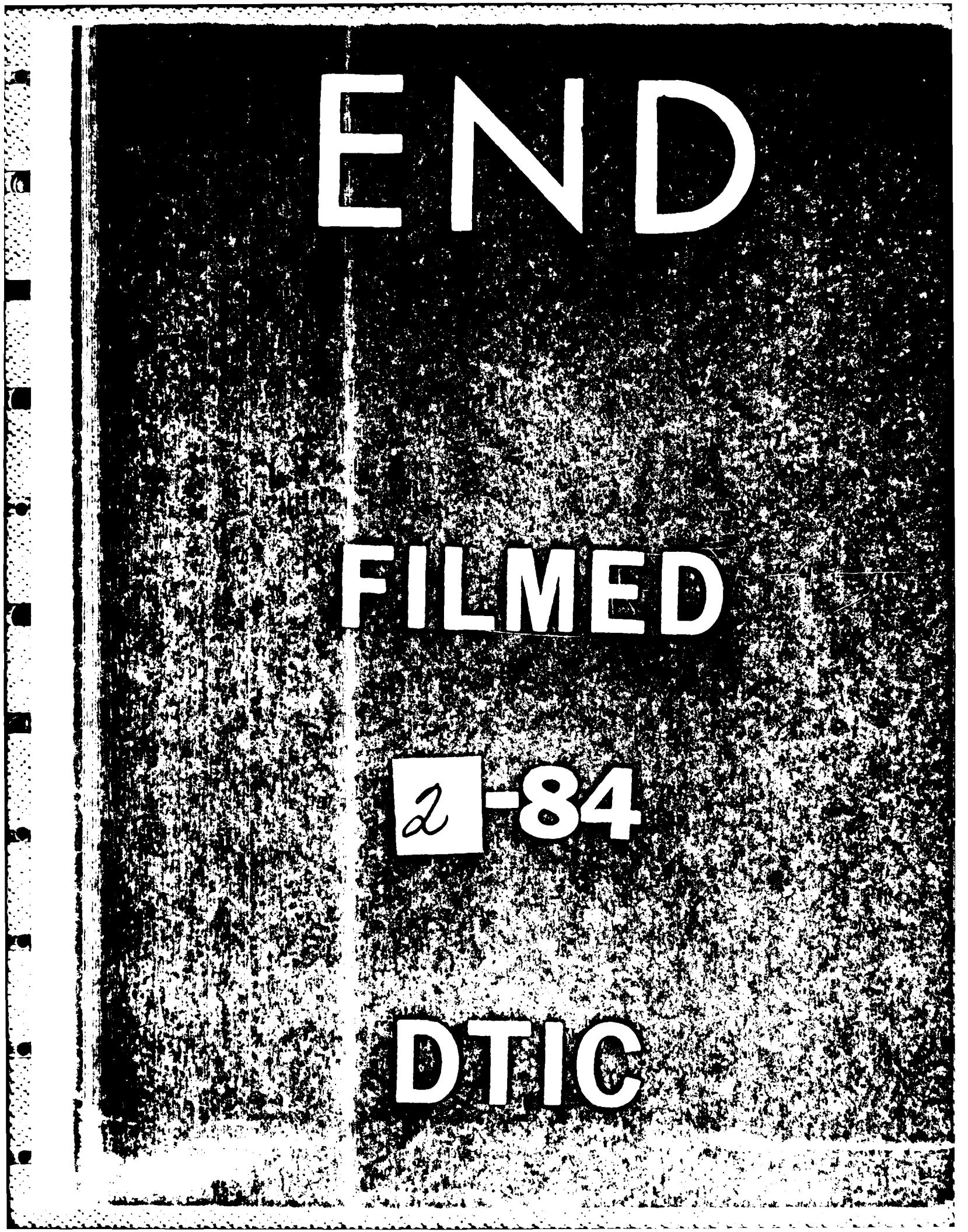
END
FILMED
2-84
DTIC